Journal of Chromatography A, 1218 (2011) 1724–1742

Contents lists available at ScienceDirect

Journal of Chromatography A

journal homepage: www.elsevier.com/locate/chroma

Contributions to reversed-phase column selectivity. I. Steric interaction

P.W. Carr[a], J.W. Dolan[b,*], U.D. Neue[c,1], L.R. Snyder[b]

[a] University of Minnesota, Minneapolis, MN, USA
[b] LC Resources, Walnut Creek, CA, USA
[c] Waters Corporation, Milford, MA, USA

ARTICLE INFO

Article history:
Received 5 October 2010
Received in revised form 16 January 2011
Accepted 17 January 2011
Available online 25 January 2011

Keywords:
Hydrophobic-subtraction
Steric interaction
Shape selectivity
Column selectivity
Retention mechanism
HPLC

ABSTRACT

In reversed-phase chromatography (RPC), the restricted retention of "bulky" solutes can occur in one of two ways, giving rise to either "shape selectivity" or "steric interaction." Starting with data for 150 solutes and 167 monomeric type-B alkylsilica columns, the present study examines the steric interaction process further and compares it with shape selectivity. The dependence of column hydrophobicity and steric interaction on column properties (ligand length and concentration, pore diameter, end-capping) was determined and compared. The role of the solute in steric interaction was found to be primarily a function of solute molecular length, with longer solutes giving increased steric interaction. We find that there are several distinct differences in the way shape selectivity and steric interaction are affected by separation conditions and the nature of the sample. Of particular interest, steric interaction exhibits a maximum effect for monomeric C_{18} columns, and becomes less important for either a C_1 or C_{30} column; shape selectivity appears unimportant for monomeric C_1–C_{18} columns at ambient and higher temperatures, but becomes pronounced for C_{30} – as well as polymeric columns with ligands $\geq C_8$. One hypothesis is that shape selectivity involves the presence or creation of cavities within the stationary phase that can accommodate a retained solute (a primarily enthalpic process), while steric interaction mainly makes greater use of spaces that pre-exist the retention of the solute (a primarily entropic process). The related dependence of hydrophobic interaction on column properties was also examined.

1. Introduction

Studies of retention in reversed-phase chromatography (RPC) have been underway for many years, based on retention measurements [1–3], spectroscopic studies [4–8], computer simulations of the stationary phase [9], and other approaches. Retention as a function of the column can be described in terms of the so-called *hydrophobic-subtraction* (H-S) model [10,11], which recognizes five separate solute–column interactions (Section 2.1). The present study examines one of these contributions to retention, so-called *steric interaction*, and compares it with what has been described as *shape selectivity* [12–16]. Additional goals of this and following studies are to learn more about the details of RPC retention, and to further evaluate the H-S model as a description of RPC retention in order to extend its possible utility. At the same time, the considerable complexity of the retention process should be kept in mind. Studies such as those reported here generally provide at best a provisional picture.

2. Background

2.1. The hydrophobic-subtraction model of reversed-phase column selectivity

The development [10,11] and application [17–21] of the hydrophobic-subtraction (H-S) model have been described. Other means for characterizing RPC column selectivity, e.g., [22–24], begin with informed assumptions about the nature of solute–stationary phase interactions, followed by the use of appropriate test-solutes to measure these interactions. The H-S model makes no such initial assumptions; it relies instead (*ab initio*) on the observed strongly linear relationships that result when values of $\log k$ for one column are plotted vs. values of $\log k$ for a second column (all other conditions the same). This behavior, as illustrated in the example of Fig. 1 for 82 of 87 test solutes (five strong bases [●] are noted as exceptions), is a consequence of a single, dominant solute-stationary phase interaction which we will refer to as *hydrophobicity* – as have others (e.g., [25,26]). If solute hydrophobicity is characterized by a value η' and column hydrophobicity by values H_1 and H_2 for columns 1 and 2, respectively, it can be argued that values of $\log k$ for a given solute should be described by $\log k_1 = a + \eta' H_1$ and $\log k_2 = a + \eta' H_2$, from which

$$\log k_1 = a\left(1 - \left[\frac{H_1}{H_2}\right]\right) + \left(\frac{H_1}{H_2}\right)\log k_2 = C_1 + C_2 \log k_2 \quad (1)$$

* Corresponding author. Tel.: +1 971 241 0946; fax: +1 503 472 4863.
E-mail address: john.dolan@lcresources.com (J.W. Dolan).
[1] Deceased.

0021-9673/$ – see front matter © 2011 Elsevier B.V. All rights reserved.
doi:10.1016/j.chroma.2011.01.047

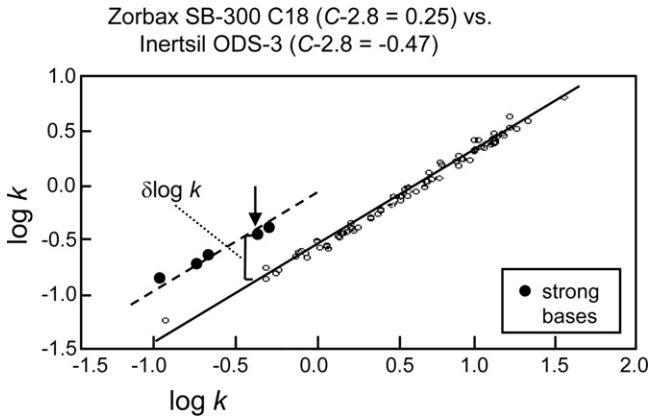

Fig. 1. Comparisons of column selectivity (log–log plots of k for two different columns) for two columns that have a relatively large difference in cation-exchange capacity (values of C-2.8). Closed circles (●) correspond to five fully protonated bases (cations).

where C_1 and C_2 are constants for specified columns 1 and 2. Resulting plots of $\log k_1$ vs. $\log k_2$ are therefore linear.

In Fig. 1, data for five protonated basic solutes (●) are observed to deviate significantly from the best-fit line through the remaining points. The size of this deviation in the example of Fig. 1 can be defined as $\delta \log k$. Assume next that the deviations $\delta \log k$ for two solutes are determined primarily by the same solute–column interaction (other than hydrophobicity, which is described by Eq. (1)). For example, fully protonated bases BH^+ can interact strongly with ionized silanols $-SiO^-$ *via* cation exchange. The contribution of a given interaction to retention can be approximated by a product of some property of the solute (in this example, its effective charge $\kappa' \approx +1$) and some property of the column (its negative charge or cation-exchange capacity C), so that for protonated solutes

$$\delta \log k \approx \kappa' C \tag{1a}$$

For solutes i and j that each obey Eq. (1a), their values of $\delta \log k$ for a given column with some value of C will be related as

$$\delta \log k_i = \left(\frac{\kappa_i}{\kappa_j}\right) \delta \log k_j \tag{1b}$$

For the same two solutes i and j, (κ_i/κ_j) will be constant, and therefore plots of $\delta \log k_i$ vs. $\delta \log k_j$ for different columns (with different values of C) should be linear with zero intercept. This is illustrated when data for the four solute pairs listed in Fig. 2 are plotted in Fig. 3a–d.

The extent to which values of $\delta \log k$ are based on a single, common solute–column interaction (other than hydrophobicity) can be assessed by the linearity of plots such as those of Fig. 3a–d – as measured by the coefficient of determination r^2. Correlations of $r^2 \approx 1$ were observed for several solute pairs, as illustrated by the examples of Fig. 3a–d. Similar plots as in Fig. 3a–d were observed for 25 of 87 solutes. Each of these 25 solutes could be assigned to one of four groups of inter-correlating solutes (groups *ii*–*v* of Fig. 2). Note that solutes from different groups are poorly correlated (Fig. 3e–h).

Solute groups *ii*–*v* each appear to represent a different solute–column interaction, provisionally identified as steric interaction (*ii*), hydrogen bonding between a basic solute and acidic column-group (*iii*), hydrogen bonding between an acidic solute and basic column-group (*iv*), and cation exchange or ion-ion interaction (*v*). The effects of hydrophobic interaction (*i*) exist for all solutes. Table 1 summarizes the results of correlations as in Fig. 3 for all 87 solutes studied. Each of these five solute–column interactions are determined by properties of the solute (η', σ', β', α', κ') and column (H, S^*, A, B, C).

The retention of most solutes will be determined by more than a single type of solute–column interaction. If these various interactions are additive (as widely assumed), retention for all solutes should be given by an equation of the form

$$\log k = \log k_{EB} + \underset{(i)}{\eta' H} - \underset{(ii)}{\sigma' S^*} + \underset{(iii)}{\beta' A} + \underset{(iv)}{\alpha' B} + \underset{(v)}{\kappa' C} \tag{2}$$

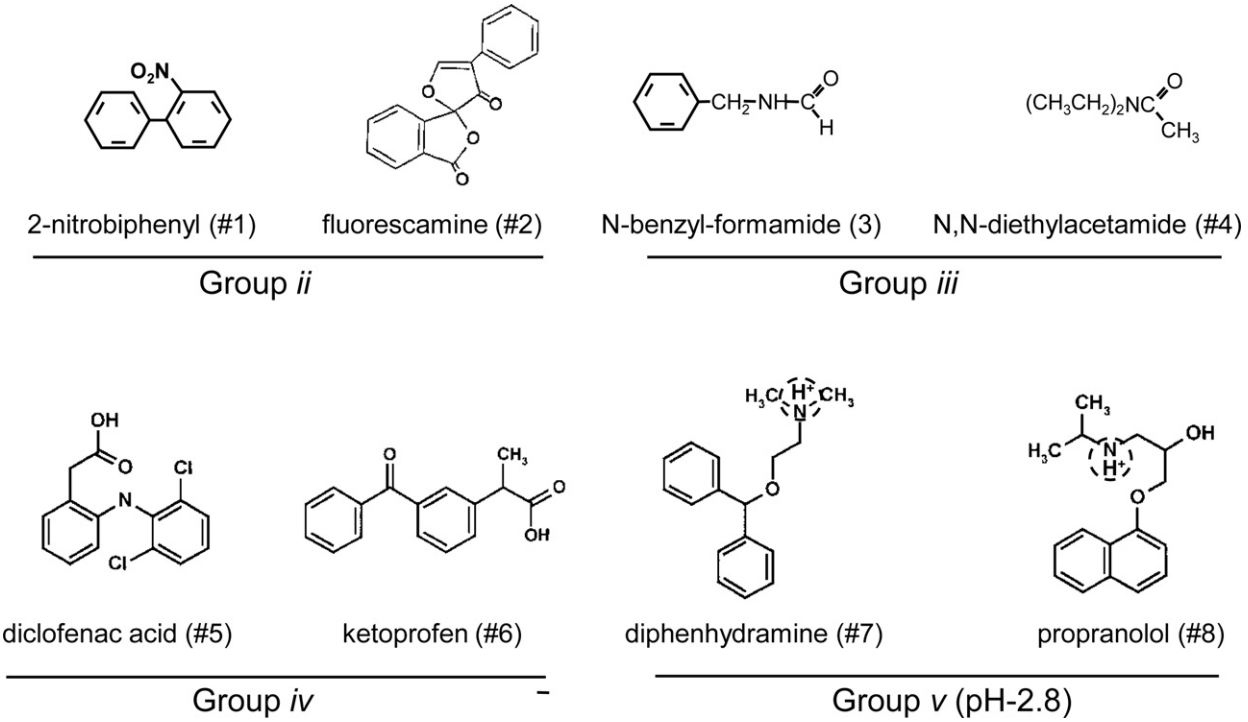

Fig. 2. Examples of solute pairs whose $\delta \log k$ values are highly correlated. (#1, 2) Group *ii*; (#3, 4) group *iii*; (#5, 6) group *iv*; (#7, 8) group *v*. Groups *ii*–*v* defined in Table 1. See text for details.

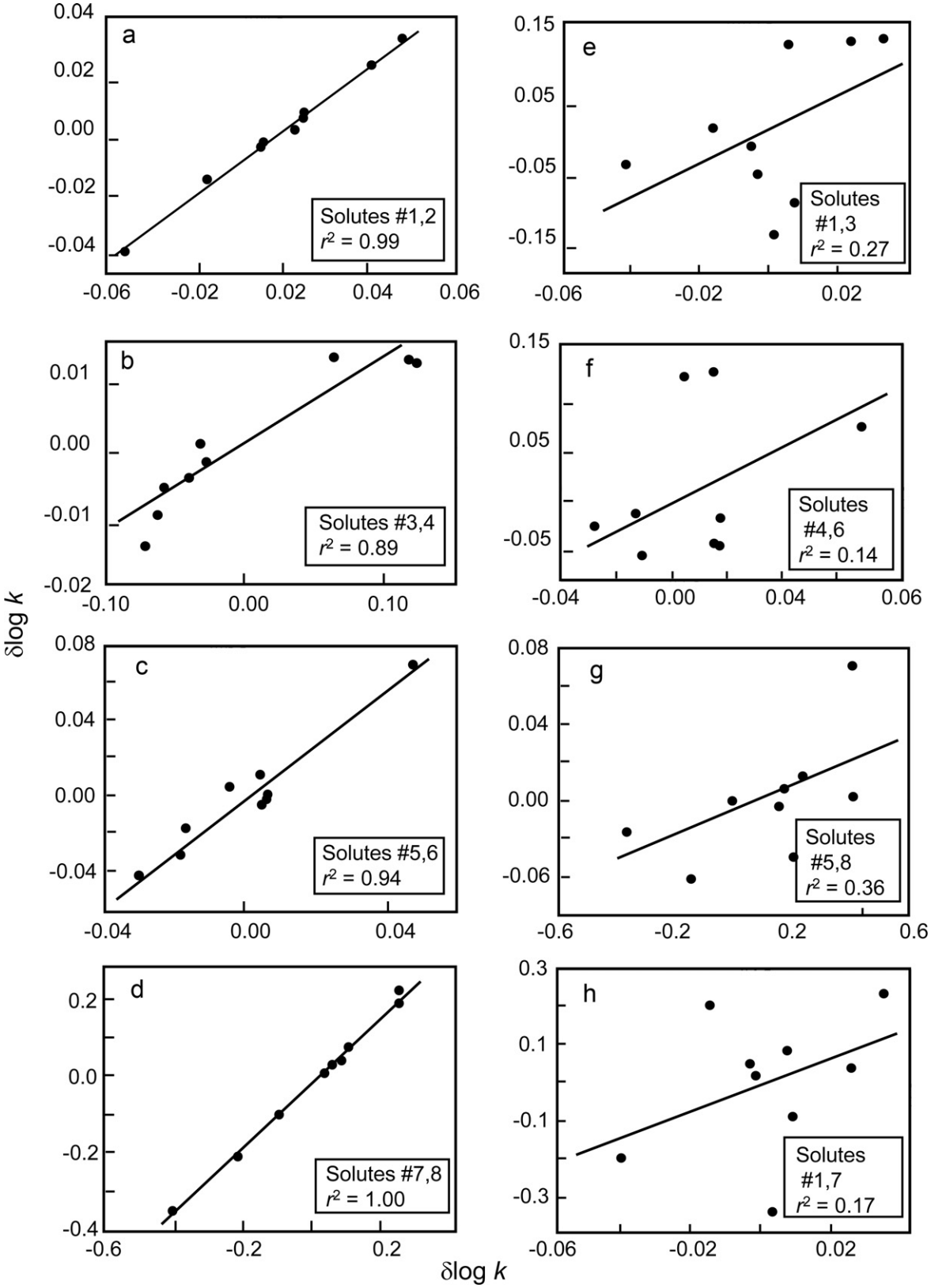

Fig. 3. Examples of plots of $\delta \log k$–$\delta \log k$ for the solute pairs of Fig. 2. Each plot represents data for nine type-B C_{18} columns described in [10,27]. Correlating solute-pairs from the same group in Fig. 2 are: (a) #1, 2; (b) #3, 4; (c) #5, 6; (d) #7, 8. Non-correlating solute-pairs from different groups are: (e) #1, 3; (f) #4, 6; (g) #5, 8; (h) #1, 7. See text for details.

Table 1
Grouping of solutes according to different solute–column interactions [11].

Group	Nature of solute	r^2 [a]	n [b]	Proposed interactions (see Eq. (2))	
				Solute[c]	Column[d]
i	All solutes	(0.99)[e]	87	η' (hydrophobicity)	H (hydrophobicity)
ii	"Bulky" molecules	0.97	12	σ' (steric hindrance)	S^* (steric hindrance)
iii	Alkyl amides	0.92	2	β' (H-B basicity)	A (H-B acidity)
iv	Non-ionized carboxylic acids	0.88	6	α' (H-B acidity)	B (H-B basicity)
v	Protonated bases	0.99	5	κ' (ionization)[f]	C (ionization)[f]

[a] Average coefficient of determination from plots of $\delta \log k$ for different solutes that fall within "similar" group (nine different columns).
[b] Number of solutes n in a correlating group.
[c] Symbol for solute property that determines the interaction in question.
[d] Symbol for column property that determines the interaction in question.
[e] Coefficient of determination of log k values for all solutes.
[f] κ' is approximately the net charge on the solute molecule (e.g., +1 for a protonated base) and C refers to the negative charge on the stationary phase (e.g., positive for columns with a net negative charge due to ionized silanols).

The quantities η', σ', β', α', and κ' correspond to properties of the solute, while H, S^*, A, B, and C represent complementary properties of the column or stationary phase (Table 1). The retention of a given solute ($\log k$) can also be related to the retention of ethyl benzene ($\log k_{EB}$), which corrects for the phase ratio of the column. For the case of type-B alkylsilica columns, Eq. (2) describes values of k with an accuracy of about ±1% [11] (2700 values of k for 150 different solutes, 90 different columns, and the same mobile phase and temperature as described in Section 3.1). For a mobile-phase pH = 2.8 and an average C_{18} column from the original study of 10 type-B columns, H will have a value of ~1.00 and values of S^*, A, B, and C will be ≈0. Note that larger values of $\sigma' S^*$ mean increased steric resistance to penetration of the solute between the bonded chains, with a corresponding decrease in retention.

The physico-chemical nature of the various solute and column parameters of Eq. (2) (Table 1) appears to be consistent with the known properties of the solutes and columns studied [11]. As an example, consider term *iii* ($\beta' A$) which is the result of hydrogen bonding between an acidic column entity (presumably a non-ionized silanol) and various non-ionized hydrogen-bond acceptor solutes, such as amines or amides. When a column is end-capped, some silanols are reacted and others are shielded by the end-capping, so that column hydrogen-bond (H-B) acidity A should decrease (as observed). Likewise, solute H-B basicity β' can be compared with a corresponding, well established solute parameter β_2 that describes solute H-B basicity in solution. Reasonable correlations exist between values of β' and β_2 for both aliphatic and aromatic solutes [11], thus supporting the conclusion that β' corresponds to solute H-B basicity.

Despite encouraging initial comparisons of interactions *i*–*v* of Eq. (2) with properties of both solutes and columns [11,27], the actual basis of these interactions merits further investigation. The present paper provides additional details on "steric interaction" (term *ii* of Eq. (2)). The nature of column hydrophobicity H has been the subject of considerable study, is less controversial, and is examined only peripherally in the present paper. Following papers will similarly consider the remaining interactions (*iii*–*v*) of Eq. (2).

2.2. Restriction of retention by steric hindrance within the stationary phase

In Section 2.1 above, so-called *steric interaction* was pointed out as one of five possible contributions to solute retention. Such a process implies that larger ("bulkier") molecules – those with larger values of σ' – experience a greater difficulty in entering the stationary phase, because they are too large to easily "fit" between alkyl ligands (steric hindrance) – thereby decreasing solute retention. Columns with larger values of S^* have more "crowded" ligands, which increase the difficulty of a solute molecule entering the stationary phase.

Three, seemingly different descriptions of steric hindrance within the stationary phase have been offered, as described in Sections 2.2.1–2.2.3. Apart from the fundamental nature of such steric hindrance, a central question is whether there is any essential difference between steric interaction ($\sigma' S^*$), as described by the H-S model, and column *shape selectivity* reported by Sander and coworkers [12–16].

2.2.1. Shape selectivity

Shape selectivity has been under investigation for the past two decades and is most pronounced for "polymeric" bonded-phases as opposed to "monomeric" columns. Polymeric columns are prepared by cross-linking the dichloro and trichloro alkylsilanes used to bond the column, and typically have higher ligand concentrations (>4 μmoles/m^2). As a result, "bulky" solute molecules find it difficult to penetrate into such stationary phases. Two solute characteristics contribute to shape-selectivity "bulkiness:" solute molecules that are (a) nonplanar, or (b) possess a wide cross section (small length-to-breadth ratio, L/B). In the case of a nonplanar molecule, its greater thickness prevents its entry into spaces between chains in the stationary-phase surface – referred to as "slots" (see the cartoon model of Fig. 4a). Similarly, wider molecules (e.g., triphenylene, right-hand side of Fig. 4b) "fit" less easily between adjacent ligands of the stationary phase than narrower molecules such as naphthacene (left-hand side of Fig. 4b). Note that the all-trans representation of ligands in the cartoon of Fig. 4b is an oversimplification, as it is well known that numerous random gauche configurations are also present [28].

Shape selectivity is commonly measured by the relative retention of non-planar tetrabenzonaphthalene (k_{TBN}) vs. that of the planar compound benzo[a]pyrene (k_{BaP}). The ratio of these two quantities $\alpha_{TBN/BaP}$ will be smaller for columns with increased shape selectivity. It will be useful in later comparisons of shape selectivity and steric interaction to express values of $\alpha_{TBN/BaP}$ in a form comparable to values of S^* (column steric interaction). The latter quantity increases with increased steric hindrance in the stationary phase, and is based on values of $\log k$, rather than k. The shape-selectivity function $\log(1/\alpha_{TBN/BaP}) \equiv \Phi_{SS}$ removes both of these differences between $\alpha_{TBN/BaP}$ and S^*, allowing a more direct comparison of these two quantities (as well as shape selectivity vs. steric interaction) for different columns or experimental conditions. However, it should be kept in mind that values of $\alpha_{TBN/BaP}$ are to some extent affected by differences in hydrophobic interaction for tetrabenzonaphthalene vs. benzo[a]pyrene, which is not the case for values of S^* (because of hydrophobic subtraction).

Shape selectivity (values of $\alpha_{TBN/BaP}$) has been measured as a function of ligand length n [12] for both monomeric and polymeric columns. It is instructive to replot these relationships as Φ_{SS} vs. n – as in Fig. 5a. For monomeric columns, there is no

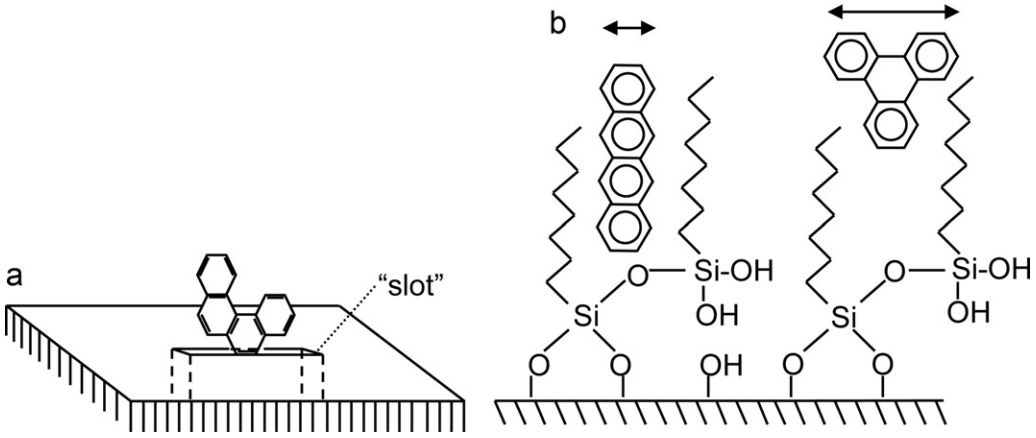

Fig. 4. Cartoon representations of shape selectivity. (a) "Slot" model; (b) preferential retention of solutes with larger length-to-breadth (L/B) ratios. See text for details.

significant change in Φ_{SS} as n increases from C_8 to C_{18}, suggesting that shape selectivity for monomeric columns is minimal for $n \leq 18$ (other experimental conditions constant, including a temperature of 35 °C). As ligand length increases beyond C_{18}, there is a marked increase in shape selectivity. For polymeric columns, shape selectivity appears minor for $n \leq C_8$, but becomes much larger for C_{18} and remains relatively constant for further increase in ligand length. The dependence of Φ_{SS} on temperature [12] (Fig. 5b) and ligand concentration C_L [14] (Fig. 5c) has also been reported. We will compare these results for shape selectivity with corresponding data for steric interaction in Sections 4.3 and 4.4.1.

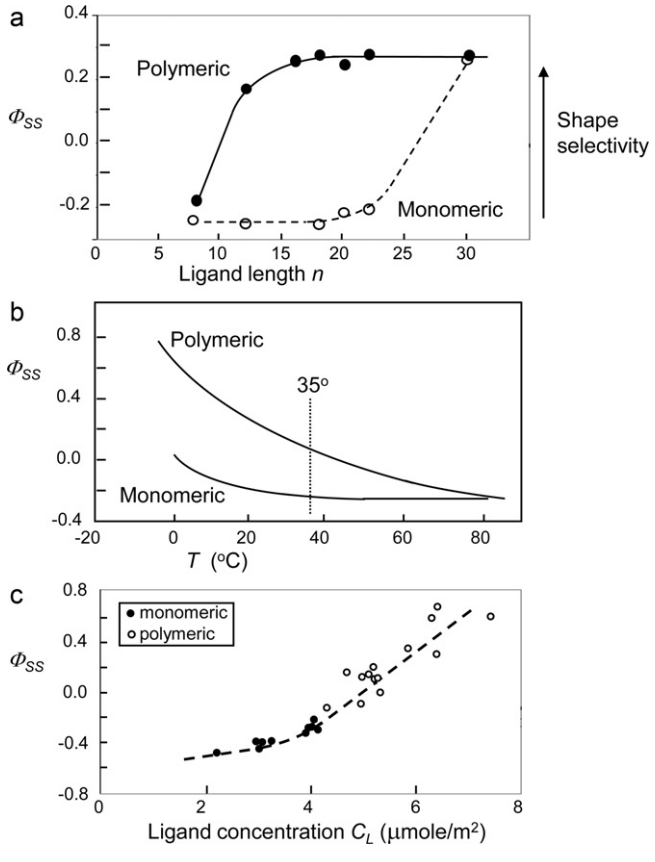

Fig. 5. Variation of shape selectivity Φ_{SS} as a function of column properties and temperature. (a) Effect of ligand length n; (b) effect of temperature; (c) effect of ligand concentration. "Monomeric" and "polymeric" refer to the nature of the stationary phase (see Section 2.2.1). Values of Φ_{SS} derived from values of $\alpha_{TBN/BaP}$ reported in [12,14]. See text for details.

2.2.2. An alternative interpretation of shape selectivity

Whereas Sander et al. originally proposed a relatively rigid stationary phase that restricts the access of bulky solute molecules to some part of the stationary phase, Siepmann and co-workers [29] later offered a somewhat modified picture on the basis of Monte Carlo simulations of the retention process. The latter studies show that low-density (i.e., monomeric) stationary phases are very flexible, so that steric exclusion results from the work required to form *transient* cavities within the stationary phase that are large enough to accept a bulky molecule. Thus larger, "bulkier" solutes will require a greater free energy to create a suitable space for the molecule within the stationary phase, meaning reduced retention. The "slot" model of Sander et al. (Fig. 4a) – on the contrary – implies pre-existing spaces of varying shapes and sizes within *high*-density stationary phases. Both the Sander and Siepmann models appear consistent with experimental data, and with each other, but for different regimes of shape selectivity (i.e., monomeric vs. polymeric columns). It seems likely that the formation of transient cavities also contributes to steric interaction to some extent, as well as to shape selectivity for polymeric columns and higher ligand concentrations.

2.2.3. Steric interaction S^*

The results of Table 1 (for type-B alkylsilica columns) in combination with the accuracy of Eq. (2) argue strongly for five different solute–column interactions. The nature of each of these distinct interactions can be inferred from the dependence of (a) solute parameters (η', σ', etc.) on solute molecular structure, and (b) column parameters (H, S^*, etc.) on column properties such as ligand length and concentration, pore diameter, and whether the column is end-capped or not (as in the above example of Section 2.1 for term *iii*: hydrogen bonding between an acceptor solute and stationary-phase silanol).

Apart from hydrophobicity (term *i*), term *ii* of Table 1 (steric interaction) is characterized by the largest number of solutes (12 from a total of 87) whose values of $\delta \log k$ are strongly correlated, as well as the second-highest average coefficient of determination ($r^2 = 0.97$). Nevertheless, the magnitude of term *ii* is much smaller than that of term *v* (cation exchange, illustrated by the strong bases [●] of Fig. 1). The smaller effect of steric interaction on retention can be seen by a similar comparison in Fig. 6a (and especially its expanded version Fig. 6b) for two columns that differ significantly in steric interaction (as measured by their values of S^*). The 12 solutes of Table 1 that exhibit pronounced steric interaction are shown in Fig. 6 as (●). Whereas the average change in k for strong bases in Fig. 1 (for two columns with significantly different values of C-2.8) was 3-fold, the corresponding change in Fig. 6 (for

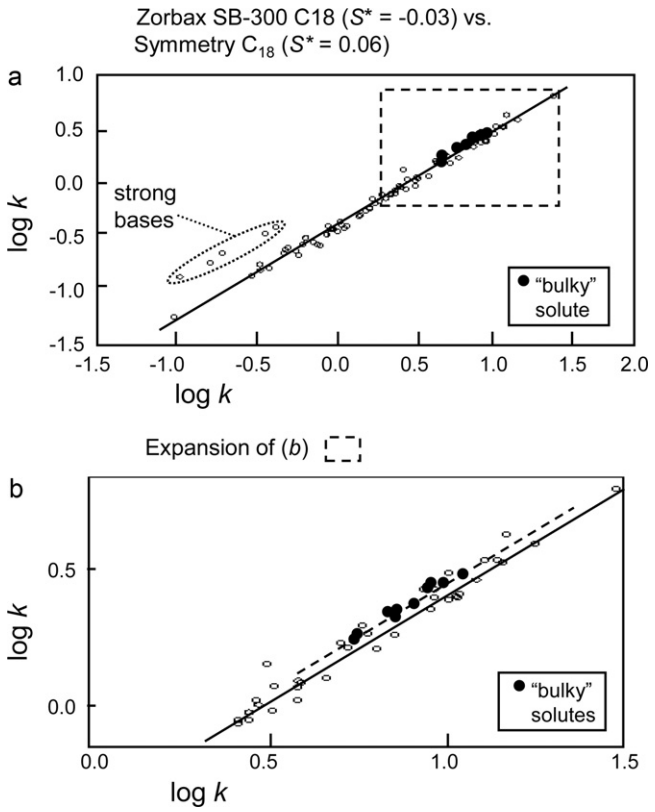

Fig. 6. Comparisons of column selectivity (log–log plots of k for two different columns). (a) Two columns with a relatively large difference in steric interaction (values of S^*); (b) expansion of (a). ● Refers to the 12 bulky solutes of Fig. 8 (those within the dashed perimeter).

two columns with very different values of S^*) is only 1.12-fold. The smaller size of the $\sigma' S^*$ term of Eq. (2), combined with experimental error, renders the interpretation of values of σ' and S^* more difficult for the $\kappa' C$ term of Eq. (2); any conclusions concerning the $\sigma' S^*$ term and steric interaction are therefore likely to be more tentative.

The nature of term *ii* of Eq. (2) was first inferred from the molecular structures of the 12 solutes whose $\delta \log k$ values are highly correlated. Each of these solutes is a relatively large molecule. Furthermore, values of σ' for all solutes were found to correlate with an approximate measure of molecular length L [27]: the number of atoms (other than hydrogen) from one end of the molecule to the other (e.g., $L = 4$ for benzene, 6 for nitrobenzene, and 6 for 2-methylnitrobenzene). Initial, limited comparisons of values of S^* with column properties suggested that S^* increases for longer stationary-phase ligands, increased ligand concentration (μmoles/m^2), narrower particle pores, and the presence of end-capping.

The increase in σ' (and decrease in term *ii*) with increasing solute length suggests a similarity between steric interaction and size-exclusion chromatography SEC (see cartoon model of Fig. 7), in that longer molecules are excluded from spaces within the particle. While in SEC long molecules are excluded from particle *pores*, steric interaction can be interpreted as partial exclusion (or restricted retention) of long molecules from the spaces between the *ligands* of the stationary phase. A further difference between SEC and RPC is that solute molecules do not interact with the stationary phase in SEC, but do in RPC. Consequently, molecular size alone will not be sufficient to result in solute exclusion from a RPC stationary phase (as would be the case in SEC; see the related discussion of [30]). As will be clear from our results and following discussion, steric interaction is a significantly more complex phenomenon than that depicted by Fig. 7b.

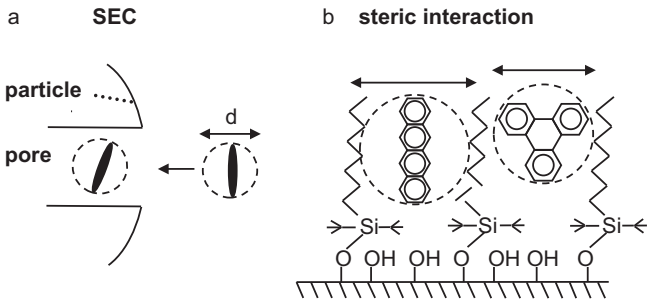

Fig. 7. Cartoon description of size-exclusion chromatography (a) and a hypothetical example of steric interaction (b); for comparison with shape selectivity in Fig. 4b. See text for details.

For both SEC and steric interaction, it has been proposed that the resulting inhibition of retention is entropic in nature (reduced degrees of freedom for the retained molecule). A major difference in these two processes (steric interaction vs. SEC) is that solutes do not interact (attractively) with the stationary phase in SEC [31], but are actively retained in RPC (mainly by hydrophobic interaction). The correlation of column shape selectivity $\alpha_{TBN/BaP}$ with steric interaction S^* is quite poor ($r^2 = 0.29$; $n = 14$), with values of S^* increasing as Φ_{SS} decreases [27] (i.e., the reverse of that expected if steric interaction and shape selectivity represent the same process).

3. Experimental

3.1. Selectivity parameters for different columns

In the present ongoing study of 167 type-B alkylsilica columns, values of the column parameters H, S^*, etc. are compared with values of the following column properties: ligand length n, pore diameter d_{pore} (nm), ligand concentration C_L (μmoles/m^2), and whether the column is end-capped or not (data of Table 2). Values of H, S^*, etc. were obtained as described in [32] ("18-solute procedure"); column properties are values reported by the manufacturer. It should be noted that different manufacturers measure these properties by different methods (no attempt is made here to rectify the results of such differences). The sample consisted of a t_0-marker (thiourea) plus 12 neutral solutes, two rather strong bases (amitriptyline, nortriptyline), a quaternary ammonium compound (berberine), and two weak acids (*n*-butylbenzoic acid, mefenamic acid); 0.5 μg of each solute was injected. The mobile phase was 50% acetonitrile/pH-2.8 buffer (30 mM potassium phosphate in the final mobile phase), the temperature was 35 °C, with a flow rate of 2.0 mL/min, and UV detection was at 205 nm. The retention of berberine was determined at both pH-2.8 and 7.0, using otherwise identical conditions. The alkylsilica columns had dimensions of 150 mm × 4.6 mm, and were packed with 5-μm particles (with a few exceptions). Values of H, S^*, etc. and related information for more than 500 RPC columns are available from the authors or at http://www.usp.org/USPNF/columns.html.

The repeatability of values of H, S^*, etc. has been evaluated for type-B alkylsilica columns [32]. Four different laboratories determined the reproducibility of these measurements, for 2–4 identical columns that were prepared from the same production batch of column packing (44 different columns were studied). The repeatability (1 std. deviation, SD) of each column parameter was as follows: H, ±0.003; S^*, ±0.001; A, ±0.022; B, ±0.001; C (pH-2.8), ±0.010; C (pH-7.0), ±0.019. Batch-to-batch repeatability has since been determined for two batches each of 11 different columns (unpublished data), with the following average repeatability (H, 0.007; S^*, 0.005; A, 0.020; B, 0.001; C (pH-2.8), 0.022; C (pH-7.0), 0.038; 1 SD). Other studies suggest that selectivity does not vary much

Table 2
Characteristics of type-B alkylsilica columns used in the present study.

#	Column	*H*	*S**	*A*	*B*	*C*-2.8	*C*-7.0	d_{pore}[a]	*n*[b]	C_L[c]	End-capped?	Source
1	Acclaim 120 C18	1.032	0.018	−0.143	−0.027	0.086	−0.002	12	18	3.20	Yes	d
2	Acclaim 120 C8	0.857	0.004	−0.274	0.011	0.086	0.016	12	8	3.70	Yes	d
3	Acclaim Polar Advantage C16	0.855	−0.068	−0.116	0.023	−0.270	0.357	12	16	2.70	Yes	d
4	Acclaim300 C18	0.957	−0.018	−0.167	0.019	0.261	0.222	30	8	3.70	Yes	d
5	ACE 300 C8	0.786	−0.003	−0.112	0.032	0.145	0.39	30	8	4.5	Yes	e
6	ACE 5 C18	1.000	0.027	−0.096	−0.007	0.143	0.096	10	18	2.60	Yes	e
7	ACE 5 C18-300	0.983	0.025	0.046	0.012	0.262	0.24	30	18	4.2	Yes	e
8	ACE 5 C18-HL	1.045	0.052	−0.088	−0.031	−0.038	−0.11	10	18	2.8	Yes	e
9	ACE 5 C4-300	0.710	−0.014	−0.183	0.039	0.166	0.36	30	4	3.7	Yes	e
10	ACE 5 C8	0.830	−0.004	−0.268	−0.017	−0.334	−0.298	10	8	3.20	Yes	e
11	ACE C4	0.674	−0.062	−0.178	0.026	0.090	0.32	10	4	2.7	Yes	e
12	Alltima C18	0.993	−0.018	0.035	−0.013	0.092	0.391	10	18	2.8	Yes	f
13	Alltima C18-LL	0.780	−0.014	−0.165	0.041	−0.056	0.367	10	18	2.3	Yes	f
14	Alltima C18-WP	0.938	0.085	0.027	0.002	−0.079	−0.081	10	18	5.2	Yes	f
15	Alltima C8	0.756	0.015	−0.279	0.009	−0.062	0.288	10	8	4.20	Yes	f
16	Alltima HP C18	0.985	−0.020	−0.040	0.006	0.177	0.199	10	18	2.6	Yes	f
17	Alltima HP C18 High Load	1.080	−0.066	0.066	−0.040	−0.322	−0.244	10	18	2.4	Yes	f
18	Alltima HP C8	0.834	0.010	−0.116	0.035	0.122	−0.42	10	8	2.5	Yes	f
19	Allure C18	1.116	0.043	0.113	−0.044	−0.047	0.067	6	18	3.60	Yes	g
20	Aqua C18	0.966	−0.030	0.033	0.009	0.068	0.276	13	18	3.70	Yes	h
21	Ascentis C18	1.077	0.058	0.030	−0.042	−0.088	−0.08	10	18	4	Yes	i
22	Ascentis C8	0.899	0.024	−0.180	−0.002	−0.124	−0.03	10	8	4.8	Yes	i
23	Ascentis Express C18	1.136	0.053	0.023	−0.052	0.067	0.11	10	18	3.5	Yes	i
24	Ascentis Express C8	0.915	0.015	−0.117	−0.005	−0.002	0.17	10	8	3.7	Yes	i
25	Atlantis dC18 b	0.917	−0.031	−0.193	0.001	0.036	0.087	10	18	1.50	Yes	j
26	Atlantis T3	0.941	−0.035	−0.181	0.006	0.029	0.71	10	18	1.65	Yes	j
27	CAPCELL C18 ACR	1.025	0.045	0.073	−0.015	0.037	0.111	12	18	2.60	Yes	k
28	CAPCELL C18 M G	1.005	0.010	0.042	−0.007	0.079	0.007	12	18	2.60	Yes	k
29	CAPCELL C18 SG120	0.987	0.031	0.093	−0.023	0.121	0.197	12	18	2.60	Yes	k
30	CAPCELL C18 UG120	1.007	0.036	0.037	−0.012	0.016	0.001	12	18	2.60	Yes	k
31	Capcell Pak C18 IF, 2 μm	0.957	0.025	−0.201	−0.001	−0.206	−0.010	12	18	2.60	Yes	k
32	Capcell Pak C18 MGII	1.011	0.011	0.047	−0.006	0.007	−0.009	12	18	2.60	Yes	k
33	CAPCELL PAK C8 DD	0.836	0.020	−0.154	0.015	−0.111	−0.08	12	8	4.8	Yes	k
34	CAPCELL PAK C8 UG120	0.854	0.037	−0.097	−0.013	−0.046	0.00	12	8	4.2	Yes	k
35	Chromegabond WR C8	0.855	0.025	−0.279	0.024	0.200	0.144	12	8	3.50	Yes	l
36	Chromolith RP18e	1.003	0.029	0.008	−0.014	0.103	0.187	13	18	3.60	Yes	m
37	Clipeus C18	1.002	0.003	−0.043	−0.010	0.079	0.34	12	18	3.4	Yes	n
38	Clipeus C8	0.822	−0.014	−0.180	0.023	0.095	0.24	12	8	4.0	Yes	n
39	Cogent HPS C18	1.021	−0.011	−0.071	−0.014	0.106	0.09	10	18	3.9	Yes	o
40	Cogent hQ C18	0.908	−0.066	0.377	0.005	0.190	2.18	10	18	3.7	No	o
41	COSMOSIL AR-II	1.017	0.011	0.126	−0.029	0.116	0.494	12	18	3.40	Yes	p
42	COSMOSIL MS-II	1.031	0.042	−0.132	−0.014	−0.118	−0.027	12	18	2.80	Yes	p
43	DeltaPak C18 100A	1.028	0.019	−0.018	−0.011	−0.051	0.024	10	18	3.00	Yes	j
44	DeltaPak C18 300A	0.955	−0.013	−0.105	0.016	0.235	0.286	30	18	3.20	Yes	j
45	Denali (120A C18)	1.052	0.042	0.125	−0.014	0.143	0.22	12	18	4.0	Yes	q
46	Develosil C30-UG-5	0.976	−0.036	−0.196	0.011	0.158	0.176	14	30	1.80	Yes	r
47	Develosil ODS-HG-5	0.980	0.015	−0.172	−0.008	0.187	0.221	10	18	3.40	Yes	r
48	Develosil ODS-MG-5	0.963	−0.036	−0.165	−0.003	−0.012	0.051	14	18	1.60	Yes	r
49	Develosil ODS-UG-5	0.996	0.025	−0.146	−0.004	0.150	0.155	14	18	3.20	Yes	r
50	Discovery BIO Wide pore 18	0.836	0.014	−0.254	0.028	0.121	0.119	30	18	3.60	Yes	i
51	Discovery BIO Wide pore C5	0.654	−0.019	−0.305	0.029	0.091	0.22	30	5	4.50	Yes	i
52	Discovery BIO Wide pore C8	0.839	0.018	−0.224	0.034	0.206	0.194	30	8	4.00	Yes	i
53	Discovery C18	0.984	0.027	−0.128	0.004	0.176	0.153	18	18	3.00	Yes	i
54	Discovery C8	0.832	0.011	−0.238	0.029	0.119	0.143	18	8	3.40	Yes	i
55	Epic C18	0.950	−0.027	−0.203	−0.007	−0.131	−0.04	11	18	3.3	Yes	l
56	Epic C4	0.779	0.019	−0.315	−0.004	−0.200	0.06	12	4	5.9	Yes	l
57	Epic C8	0.893	0.022	−0.194	−0.001	−0.102	0.04	12	8	5.5	Yes	l
58	Gemini C18 110A	0.967	−0.008	0.027	0.013	−0.091	0.19	11	18	2.2	Yes	h
59	Halo-C18	1.107	0.048	0.006	−0.050	0.056	0.629	9	18	3.50	Yes	s
60	Halo-C8	0.913	0.028	−0.132	−0.008	−0.011	0.588	9	8	3.70	Yes	s
61	Hichrom RPB	0.964	0.027	0.106	0.003	0.153	0.14	15	13	2.0	Yes	t
62	Hypersil Beta Basic-18	0.993	0.033	−0.099	0.001	0.163	0.126	15	18	3.60	Yes	u
63	Hypersil Beta Basic-8	0.834	0.016	−0.248	0.029	0.110	0.115	15	8	3.90	Yes	u
64	Hypersil BetamaxNeutral	1.098	0.036	0.067	−0.031	−0.038	0.012	6	8	3.00	Yes	u
65	Hypersil Bio Basic-18	0.974	0.025	−0.100	0.007	0.253	0.217	30	18	4.90	Yes	u
66	Hypersil Bio Basic-4	0.691	−0.009	−0.191	0.032	0.188	0.39	30	4	9.2	Yes	u
67	Hypersil Bio Basic-8	0.821	0.012	−0.233	0.029	0.231	0.210	30	8	5.6	Yes	u
68	Hypersil GOLD	0.881	0.002	−0.017	0.036	0.162	0.479	18	18	3.30	Yes	u
69	Hypersil GOLD C8	0.825	0.016	−0.157	0.030	0.093	0.215	18	8	4.00	Yes	u
70	Hypurity C18	0.980	0.025	−0.091	0.003	0.192	0.167	19	18	3.00	Yes	u
71	HyPurity C4	0.713	0.000	−0.291	0.028	0.121	0.252	19	4	4.70	Yes	u
72	Hypurity C8	0.833	0.011	−0.201	0.035	0.157	0.161	19	8	4.00	Yes	u
73	Inertsil C8-3	0.830	−0.004	−0.268	−0.017	−0.334	−0.362	10	8	1.60	No	v
74	Inertsil ODS-2	1.007	0.045	−0.079	−0.014	−0.139	0.446	10	18	3.20	Yes	v
75	Inertsil ODS-3	0.990	0.022	−0.146	−0.023	−0.474	−0.334	10	18	1.30	Yes	v
76	Inertsil WP300 C18	0.938	−0.015	−0.117	0.001	0.202	0.16	30	18	2.0	Yes	v

Table 2
(*Continued*).

#	Column	*H*	*S**	*A*	*B*	*C*-2.8	*C*-7.0	d_{pore}[a]	*n*[b]	C_L[c]	End-capped?	Source
77	Inertsil WP300 C8	0.793	−0.015	−0.212	0.013	0.122	0.07	30	8	3.0	Yes	v
78	J'Sphere H80	1.132	0.059	−0.023	−0.068	−0.242	−0.161	8	18	2.90	Yes	j
79	J'Sphere L80	0.762	−0.036	−0.216	−0.001	−0.400	0.345	8	18	0.90	Yes	j
80	J'Sphere M80	0.926	−0.026	−0.123	−0.004	−0.294	0.139	8	18	1.60	Yes	j
81	Jupiter300 C18	0.945	0.031	−0.225	0.008	0.234	0.218	30	18	5.50	Yes	h
82	Jupiter300 C4	0.698	0.008	−0.426	0.019	0.152	0.141	30	4	6.30	Yes	h
83	Jupiter300 C5	0.729	0.021	−0.382	0.016	0.129	0.33	30	5	5.30	Yes	h
84	Kromasil 100-5C18	1.051	0.036	−0.071	−0.023	0.039	−0.057	11	18	3.50	Yes	w
85	Kromasil 100-5C4	0.733	0.003	−0.335	0.015	0.009	−0.004	11	4	3.80	Yes	w
86	Kromasil 100-5C8	0.864	0.013	−0.213	0.019	0.054	−0.001	11	8	3.70	Yes	w
87	Luna C18	1.018	0.025	0.072	0.008	−0.361	−0.04	10	18	2.9	Yes	j
88	Luna C18(2)	1.002	0.024	−0.124	−0.007	−0.269	−0.174	10	18	3.4	Yes	j
89	Luna C5	0.800	0.035	−0.252	0.003	−0.278	0.11	10	5	7.90	Yes	j
90	Luna C8	0.875	0.037	−0.015	0.024	−0.400	0.133	10	8	4.9	Yes	j
91	Luna C8(2)	0.889	0.041	−0.222	−0.001	−0.300	−0.17	10	8	4.2	Yes	j
92	Nucleodur C18 Gravity	1.056	0.041	−0.097	−0.025	−0.080	0.32	11	18	3.3	Yes	x
93	Nucleodur C8 Gravity 5 micron	0.868	0.032	−0.240	0.000	−0.158	0.63	11	8	4.2	Yes	x
94	Nucleodur Isis	1.023	0.055	−0.078	−0.029	−0.019	0.15	11	18	3.8	Yes	x
95	Nucleodur Pyramid	0.958	0.003	−0.130	−0.016	−0.289	0.21	11	18	2.4	Yes	x
96	Nucleodur Sphinx RP	0.805	−0.071	−0.274	0.000	0.022	0.72	11	18	2.6	Yes	x
97	OmniSpher 5 C18	1.055	0.051	−0.033	−0.029	0.122	−0.167	11	18	3.50	Yes	y
98	PRECISION C18	1.002	0.003	−0.042	−0.010	0.079	0.341	12	18	2.80	Yes	z
99	PRECISION C8	0.821	−0.014	−0.180	0.022	0.095	0.241	12	8	3.10	Yes	z
100	Prodigy ODS (3)	1.023	0.025	−0.131	−0.012	−0.195	−0.134	10	18	3.30	Yes	h
101	Prodigy ODS(2)	0.995	0.030	−0.114	−0.001	−0.091	0.24	10	18	3.8	Yes	h
102	Prontosil 120-3-C30	0.919	−0.130	0.571	−0.003	0.51	1.79	12	30	2.9	No	aa
103	ProntoSIL 120-5 C18 SH	1.031	0.018	−0.109	−0.024	0.113	0.402	12	18	3.00	Yes	aa
104	ProntoSIL 120-5 C8 SH	0.739	−0.062	−0.081	0.013	0.076	0.526	12	8	3.20	Yes	aa
105	Prontosil 120-5-C1	0.413	−0.079	−0.085	0.020	0.042	0.66	12	1	6.3	No	aa
106	ProntoSIL 120-5-C18 H	1.005	0.008	−0.106	−0.004	0.125	0.156	12	18	2.90	Yes	aa
107	ProntoSIL 120-5-C18-AQ	0.973	−0.007	−0.082	0.004	0.137	0.224	12	18	2.10	Yes	aa
108	ProntoSIL 200-5 C8 SH	0.761	−0.026	−0.195	0.024	0.125	0.238	20	8	3.20	Yes	aa
109	Prontosil 200-5-C18 AQ	0.973	−0.011	−0.057	0.006	0.125	0.29	20	18	2.7	Yes	aa
110	ProntoSIL 200-5-C18 H	0.955	−0.001	−0.121	0.016	0.163	0.218	20	18	2.90	Yes	aa
111	Prontosil 200-5-C30	0.909	−0.099	0.347	0.007	0.31	1.17	20	30	3.8	No	aa
112	Prontosil 200-5-C4	0.549	−0.063	−0.221	0.038	0.086	0.51	20	4	5.9	No	aa
113	ProntoSIL 300-5 C8 SH	0.739	−0.041	−0.131	0.028	0.156	0.405	30	18	3.20	Yes	aa
114	ProntoSIL 300-5-C18 H	0.956	−0.012	−0.090	0.015	0.238	0.249	30	18	2.90	Yes	aa
115	Prontosil 300-5-C30	0.893	−0.107	0.322	0.030	0.40	1.55	30	30	4.4	No	aa
116	Prontosil 300-5-C30 EC	0.925	−0.047	−0.018	0.012	0.30	0.46	30	30	4.4	Yes	aa
117	Prontosil 300-5-C4	0.471	−0.093	−0.074	0.055	0.12	0.79	30	4	4.0	No	aa
118	ProntoSIL 60-5 C8 SH	0.929	−0.015	0.161	−0.017	−0.313	1.005	6	8	3.20	Yes	aa
119	ProntoSIL 60-5-C18 H	1.158	0.041	0.066	−0.078	0.102	0.263	6	18	2.90	Yes	aa
120	Prontosil 60-5-C4	0.686	−0.072	0.108	0.001	−0.056	1.20	6	4	2.6	No	aa
121	Purospher STAR RP18e	1.003	0.013	−0.071	−0.037	0.018	0.044	12	18	3.00	Yes	m
122	Restek Ultra C18	1.055	0.030	−0.069	−0.022	0.009	−0.066	10	18	3.60	Yes	g
123	Restek Ultra C8	0.876	0.031	−0.229	0.018	0.043	0.012	10	8	3.60	Yes	g
124	SepaxBioC18	0.915	−0.028	−0.157	0.019	0.227	0.24	30	18	2.9	Yes	ab
125	SepaxBio-C4	0.663	−0.014	−0.291	0.022	0.109	0.23	30	4	4.0	Yes	ab
126	SepaxBio-C8	0.774	−0.025	−0.272	0.025	0.164	0.22	30	8	3.2	Yes	ab
127	Symmetry 300 C18	0.984	0.031	−0.051	0.003	0.228	0.202	30	18	3.50	Yes	j
128	Symmetry 300 C4	0.659	−0.016	−0.428	0.014	0.101	0.184	30	4	3.20	Yes	j
129	Symmetry C18	1.052	0.063	0.018	−0.021	−0.302	0.123	9	18	3.20	Yes	j
130	Symmetry C_8	0.893	0.049	−0.205	0.021	−0.509	0.283	9	8	3.50	Yes	j
131	Synergi Max-RP	0.989	0.028	−0.008	−0.013	−0.133	−0.034	8	18	3.20	Yes	h
132	Targa C18	0.977	−0.019	−0.070	0.000	0.013	0.18	12	18	2.7	Yes	n
133	TSKgel Octyl-80Ts	0.814	−0.005	−0.253	0.017	0.089	0.46	8	18	1.7	Yes	ac
134	TSKgel ODS-100V	0.901	−0.043	−0.226	−0.009	−0.060	−0.02	10	18	1.8	Yes	ac
135	TSKgel ODS-100Z	1.032	0.018	−0.135	−0.031	−0.064	−0.16	10	18	2.6	Yes	ac
136	TSK-GEL ODS-140HTP	1.002	0.051	−0.251	−0.032	0.134	0.14	14	18	2.7	Yes	ac
137	TSKgel ODS-80Ts	0.971	−0.015	−0.132	−0.004	0.010	0.29	8	18	1.7	Yes	ac
138	TSKgel ODS-80Ts QA	0.940	−0.030	−0.118	0.005	0.004	0.36	8	18	1.7	Yes	ac
139	TSKgel Super-Octyl	0.824	0.034	−0.155	0.010	0.126	0.23	11	8	5.1	Yes	ac
140	TSKgel Super-ODS	0.998	0.030	−0.048	−0.019	0.154	0.24	11	18	2.7	Yes	ac
141	Ultracarb ODS (30)	1.114	0.016	0.377	−0.050	−0.311	0.73	6	18	1.6	Yes	h
142	Vision C18 HL	1.056	0.029	0.018	0.015	0.245	0.30	12	18	2.2	Yes	f
143	Wakosil 5C8RS	0.802	−0.008	−0.272	0.001	−0.117	0.10	12	18	3.6	Yes	ad
144	Wakosil II 5C18AR	0.998	0.075	−0.055	−0.034	0.070	0.01	12	18	4.3	Yes	ad
145	Wakosil II 5C18HG	1.039	0.036	0.015	−0.023	0.009	0.21	12	18	3.0	Yes	ad
146	Wakosil II 5C18RS	0.964	−0.008	−0.160	−0.009	−0.070	0.05	12	18	3.0	Yes	ad
147	XBridge C18	1.007	0.028	−0.097	0.009	0.178	0.138	14	18	3.10	Yes	j
148	Xterra MS C18	0.984	0.012	−0.143	−0.015	0.133	0.051	13	18	2.20	Yes	j
149	Xterra MS C8	0.803	0.005	−0.293	−0.005	0.058	−0.009	13	8	2.70	Yes	j
150	YMC Hydrosphere C18	0.937	−0.022	−0.129	0.006	−0.139	0.16	13	18	1.3	Yes	j

Table 2
(*Continued*).

#	Column	*H*	*S**	*A*	*B*	*C*-2.8	*C*-7.0	d_{pore}[a]	*n*[b]	C_L[c]	End-capped?	Source
151	YMC ODS-AQ	0.965	−0.036	−0.135	0.004	−0.068	0.10	13	18	2.4	Yes	j
152	YMC Pack Pro C18 RS	1.114	0.057	−0.061	−0.056	−0.176	−0.22	13	18	2.8	Yes	j
153	YMC Pro C18	1.015	0.014	−0.120	−0.007	−0.155	−0.006	13	18	2.50	Yes	j
154	YMC Pro C8	0.890	0.014	−0.215	0.007	−0.323	0.019	13	8	3.20	Yes	j
155	Zorbax Eclipse Plus C18	1.030	0.007	−0.072	−0.020	−0.004	0.02	10	18	1.3	Yes	ae
156	Zorbax Eclipse Plus C8	0.889	0.017	−0.172	−0.005	−0.042	0.05	10	8	2.1	Yes	ae
157	Zorbax Eclipse XDB-C18	1.077	0.024	−0.063	−0.033	0.055	0.088	8	18	4.00	Yes	ae
158	Zorbax Eclipse XDB-C8	0.919	0.025	−0.219	−0.008	0.003	0.012	8	8	3.80	Yes	ae
159	Zorbax Extend C18	1.098	0.050	0.012	−0.041	0.030	0.02	8	18	3.9	Yes	ae
160	Zorbax Rx-18	1.077	0.037	0.309	−0.038	0.096	0.415	8	18	3.50	No	ae
161	Zorbax Rx-C8	0.792	−0.076	0.116	0.018	0.012	0.948	8	8	2.00	No	ae
162	Zorbax StableBond 300A C18	0.905	−0.050	0.045	0.043	0.254	0.701	30	18	2.00	No	ae
163	Zorbax StableBond 300A C3	0.526	−0.122	−0.195	0.047	0.057	0.36	30	3	2.00	No	ae
164	Zorbax StableBond 300A C8	0.701	−0.085	0.002	0.047	0.146	0.820	30	8	2.00	No	ae
165	Zorbax StableBond 80A C18	0.996	−0.032	0.264	−0.001	0.136	1.041	8	18	2.00	No	ae
166	Zorbax StableBond 80A C3	0.601	−0.124	−0.081	0.038	−0.084	0.81	8	3	2.00	No	ae
167	Zorbax StableBond 80A C8	0.795	−0.079	0.137	0.018	0.014	1.020	8	8	2.00	No	ae

d, Dionex; e, ACT; f, Grace-Alltech; g, Restek; h, Phenomenex; i, Supelco; j, Waters; k, Shiseido; l, ES Industries; m, Merck; n, Higgens; o, MicroSolve; p, Nacalai Tesque; q, Grace-Vydac; r, Nomura; s, Advanced Materials Technology; t, HiChrom; u, Thermo/Hypersil; v, GL Science; w, Akzo Nobel; x, Macherey Nagel; y, Varian; z, MacMod; aa, Bischoff; ab, Sepax Technologies; ac, Tosoh; ad, SGE; ae, Agilent.

[a] Pore diameter (nm).

[b] Ligand length (e.g., 18 for a C_{18} column).

[c] Ligand concentration (μmoles/m^2).

among nominally equivalent virgin columns from different production batches [33], in agreement with the latter data.

3.2. Correlations of column selectivity parameters with column properties

Multiple regressions were carried out for values of *H* or *S** vs. a polynomial of various column properties (ligand length *n* and concentration C_L, pore diameter d_{pore}, end-capping); e.g., for values of *H*

$$H = a + \underbrace{bn + cn^2}_{\text{ligand length}} + \underbrace{dd_{pore} + ed_{pore}^2}_{\text{pore diameter}} + \underbrace{fC_L + gC_L^2}_{\text{ligand concentration}} + \underbrace{hE_C}_{\text{end capping}} \quad (3)$$

Values of the various coefficients *a*, *b*, ..., *h* result from the regression. E_C has a value of one if the column is end-capped, and zero if not end-capped; the value of *h* thus represents the quantitative effect on *H* of end-capping. An identical relationship as Eq. (3) was also used in this study to determine the effects of column properties on *S** (*S** replacing *H*). Preliminary information of this kind had been reported for a small number of columns [11], but the present study based on 167 columns was found to provide more representative and detailed conclusions.

4. Results and discussion

The aim of the present study is to both test and extend previous conclusions about steric interaction, by means of a further examination of values of the solute-parameter σ' (Section 4.1) and column-parameter *S** (Section 4.2). We have values of σ' for 150 different solutes (as measured by means of Eq. (2) [10,27]) which can be compared with solute molecular structure. Similarly, values of *S** were measured for 167 type-B alkylsilica columns, for use with values of their column properties as supplied by the manufacturer (Table 2). In view of a relatively large literature that deals with shape selectivity, and because both shape selectivity and steric interaction arise from steric hindrance in the stationary phase, a detailed comparison of these two phenomena was attempted (Section 4.3).

4.1. Values of σ' as a function of solute molecular structure

Values of σ' suggest that term *ii* of Eq. (2) ($\sigma' S^*$) is the result of partial exclusion of "large" molecules from the stationary phase; i.e., those with longer molecular length *L*. This contrasts with shape selectivity, where solute "bulkiness" is determined by molecular planarity and the ratio of length to width (with retention favored for relatively longer molecules of similar molecular weight). Solutes whose retention is primarily determined by steric (as well as hydrophobic) interaction will have $\delta \log k$ values that are highly correlated (Section 2.1 and Table 1); Fig. 8 summarizes those solutes of group *ii* with values of $r^2 \geq 0.90$ (17 solutes vs. 12 in Table 1 with $r^2 \geq 0.97$). Hydrocarbons (because of their relative non-polarity) represent a second class of solutes that should be largely free of interactions other than steric and hydrophobic. Note that a coefficient of determination $r^2 < 0.9$ for smaller nonpolar solutes (e.g., most C_1–C_4 alkylbenzenes) is the likely result of their smaller values of σ' combined with experimental error, rather than contributions from other solute–column interactions (i.e., terms *iii*–*v* of Eq. (2)). Solutes from the latter two solute groups (hydrocarbons and Fig. 8) are most likely to have minimum contributions from interactions *iii*–*v* of Eq. (2), and should in principle best define the dependence of σ' on *L* – as illustrated in Fig. 9. These data can be fit by an empirical relationship over the limited range in *L* ($4 \leq L \leq 14$) for which we have data:

$$\sigma' = -1.301 + 0.297L - 0.009L^2 \quad (r^2 = 0.87; \text{SD} = 0.17) \quad (4)$$

Comparisons of values of σ' from different sources suggest an experimental uncertainty in σ' of $\sim\pm0.1$ unit. The somewhat larger error in Eq. (4) (SD = 0.17) likely arises from contributions to σ' other than solute length *L* (see Section 4.1.1), as well as the estimation of length *L* by the number of atoms in a continuous line (necessarily approximate, as inter-atomic distances vary somewhat, and hydrogen atoms are ignored). Consequently, the observed imprecision of Eq. (4) (±0.17) appears reasonable. Compared to the nonpolar hydrocarbon solutes of Fig. 9 (○), the highly correlated solutes (●) are more polar and have generally higher values of σ'. This suggests that solute polarity might also contribute to values of σ', a possibility that is tested in Fig. 10a by comparing values of σ' for various polar-substituted benzenes with the correlation of Fig. 9 (Eq. (4)). There is no overall bias of these data relative to Eq. (4), deviations

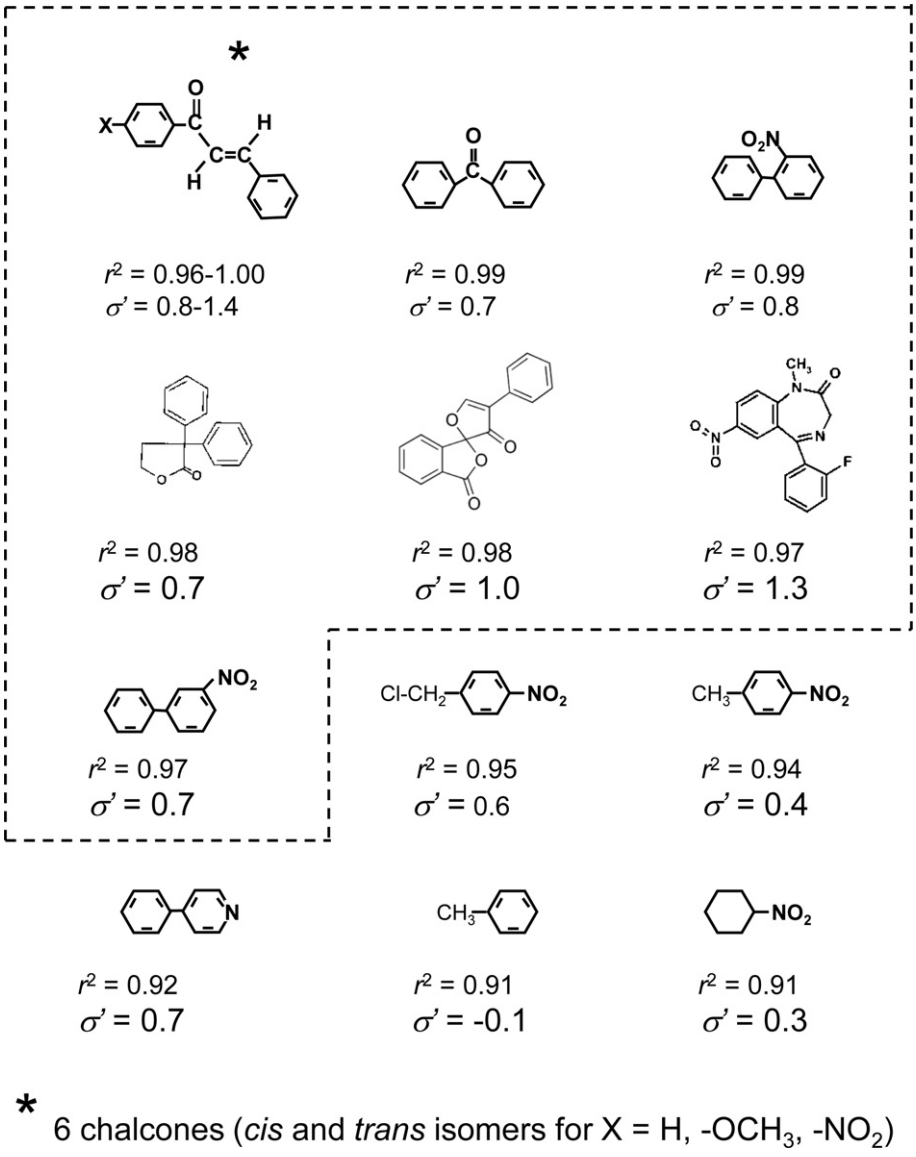

Fig. 8. Solutes of group *ii* (Table 1) whose $\delta \log k$ values are highly correlated. Correlations for each solute are vs. average values of $\delta \log k$ for the first seven solutes of the figure (six *cis*- and *trans*-chalcones [marked by *] plus benzophenone). The 12 solutes of Table 1 (group *ii*) are inside the dashed perimeter.

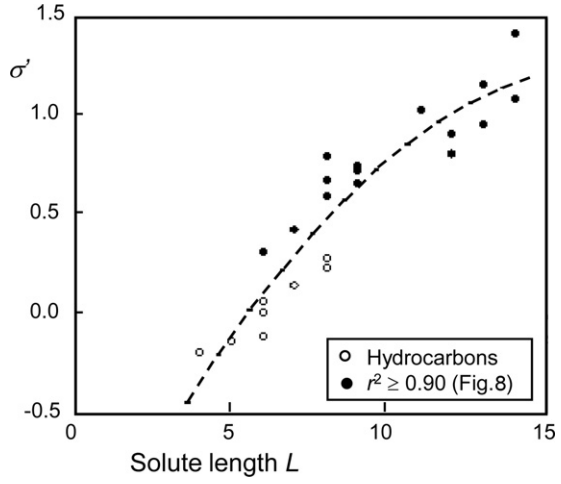

Fig. 9. Correlation of values of σ' with solute molecular length *L*. Data for nonpolar aromatic hydrocarbons (○) and the (highly correlated) solutes from Fig. 8 (●).

in the plot do not correlate with common measures of solute polarity, and the scatter is less (SD = 0.13) for the data of Fig. 10a than for Fig. 9 (where SD = 0.17). For the solutes of Figs. 8 and 10a, we conclude that solute polarity does not *per se* affect values of σ', which limits the possibilities to molecular shape and/or size (as approximated by length *L*).

A similar comparison as in Fig. 10a for polar-substituted benzenes is shown in Fig. 10b for various *n*-alkanes substituted by different polar substituents in the 1-position. A best-fit curve through these data would not differ appreciably from Eq. (4) (shown as - - -). Again, as in Fig. 10a, there is no indication of any contribution of solute polarity to values of σ'. The combined 62 solutes of Figs. 8 and 10a and b adhere to Eq. (4) with an overall accuracy of ±0.14 (1 SD) – only marginally worse than the estimated uncertainty of values of σ'. For these solutes, molecular length is clearly the major contributor to steric interaction and values of σ'.

In contrast to the results of Figs. 8 and 10a and b, values of σ' for certain other classes of solutes deviate more or less strongly from Eq. (4). Fig. 10c shows data for aliphatic alco-

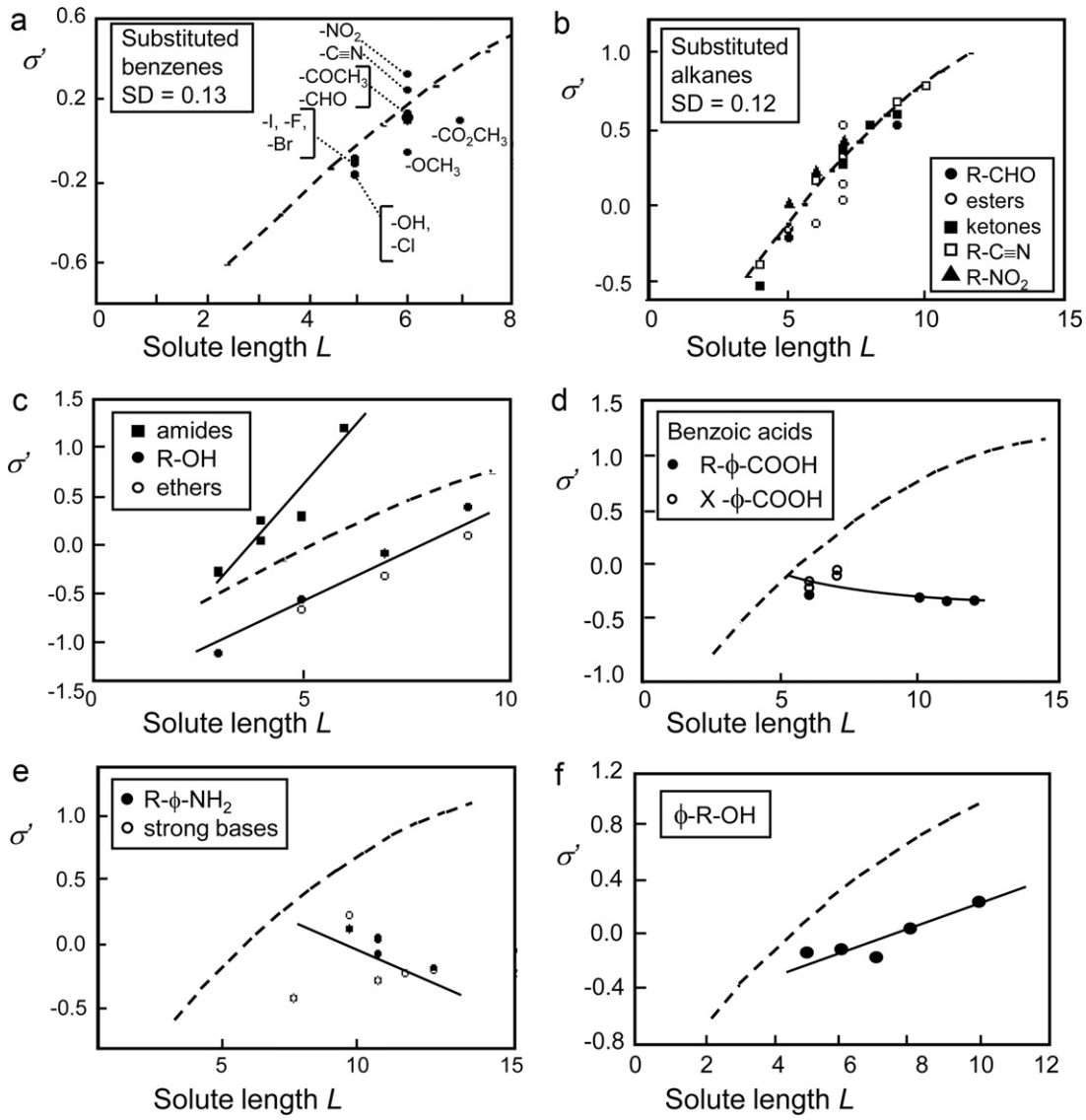

Fig. 10. Fit of σ'-values vs. solute length L for various solutes, and comparisons with the correlation of Fig. 9 (Eq. (4), shown in each case as (– – –)). (a) Benzenes substituted by various polar substituents; (b) *n*-alkanes substituted by various polar substituents in the 1-position; (c) aliphatic ethers, alcohols, and N,N-dialkylamides; (d) benzoic acids substituted by 4-*n*-alkyl groups (R), or polar substituents (X) in the *meta* or *para* position; (e) 4-*n*-alkyl-substituted anilines, and strong bases; (f) Ψ-substituted 1-alkanols; data of [10].

hols, ethers, and amides. The amides exhibit significantly higher values of σ' than predicted by Eq. (4) (- - -), while the alcohols and ethers have lower values. Even larger deviations from Eq. (4) are found for substituted benzoic acids (Fig. 10d), and various amines (Fig. 10e). Phenyl alkanols (e.g., phenol, benzyl alcohol, 2-phenylethanol) show deviations (Fig. 10f) that are similar in magnitude to those for the aliphatic alcohols of Fig. 10c.

The molecular structures of the 49 remaining solutes differ from those represented in Figs. 8 and 10; two of these solutes have σ' values that are 2-SD higher than predicted by Eq. (4), with 14 solutes that are 2-SD lower. These 16 deviating solutes include five acids, five phenols, and two amides – all solute-types that show (generally negative) deviations from Eq. (4) – similar to the behavior of related solutes in Fig. 10c and f.

Previously [11,21], the greatly reduced values of σ' observed for the ionizable solutes of Fig. 10d and e were attributed to an exclusion of the ionized acid- or base-group of the solute molecule from the nonpolar stationary phase. However, this now appears unlikely; the various benzoic acids of Fig. 10d are for the most part in the neutral form, and while the anilines of Fig. 10e are partly ionized, they are likely retained as the non-ionized molecule. There is a common feature of the various non-correlating solutes, however, in that they generally exhibit strong additional interactions with the stationary phase other than hydrophobic or steric. This is indicated by their generally larger values of β', α', or κ', as summarized in Table 3 for deviating vs. correlating (compliant) solutes. These same (polar) molecules also tend to interact with the stationary phase by hydrogen bonding or ion exchange. Such an interaction tends to "localize" the molecule within the stationary phase, which means a restriction of the molecule's mobility within the stationary phase. This should in turn result in smaller values of σ' vs. predictions by Eq. (4), as restricted molecules will be less likely to differentiate between columns with different S^* values. Solute conformation (and values of σ') might also be affected by the interaction of polar groups with the solvent that forms part of the stationary phase, however the data of Fig. 10a for more polar solutes such as phenol suggest otherwise.

Table 3
Contributions to σ' other than length, based on deviations $\delta\sigma'$ of experimental values from values of Eq. (4). Data of [10,27].

Solute type	Avg. values of each solute parameter (other than η' or σ')		
	β'	α'	κ'
Compliant solutes (Figs. 8 and 10a and b)			
Average values	0.01	0.07	−0.02
std. deviation	0.08	0.08	0.02
Deviating solutes (avg. values)			
Amides	0.70	0.05	0.03
ROH	0.18	n.d.	n.d.
Ethers	0.24	n.d.	n.d.
Benzoic acids	0.01	1.11	−0.05
Strong bases	0.00	0.00	1.00
Anilines	0.07	0.17	0.09
Phenyl alkanols	0.04	0.13	0.02

Other features of the solute molecule	$\delta\sigma'$[a]	
	avg	SD
"Thick"[b]	+0.14	0.08
Para ϕ-X_2[c]	−0.26	0.04
Tertiary substituents[d]	0.26	0.03

[a] Experimental value of σ' minus value from Eq. (4).
[b] Four solutes from Fig. 7 of [11].
[c] *p*-Xylene, 4-chlorotoluene, 4-bromotoluene, *p*-dichlorobenzene.
[d] *t*-Butylbenzene, benzotrichloride.

4.1.1. Other contributions to σ'

Figs. 9 and 10 summarize values of σ' as a function of L for relatively "simple" molecules. We can define a contribution to σ' other than length as $\delta\sigma'$, equal to the experimental value of σ' minus the value from Eq. (4). Previously [27] it was asserted that certain 3-dimensionally "thick" molecules (e.g., fluorescamine, ferrocene) exhibit somewhat larger values of σ' than expected. This observation has since been reexamined by means of Eq. (4), as summarized at the bottom of Table 3. For four such "thick" molecules, the average increase in σ' ($\delta\sigma'$) was only +0.14 – a marginally significant contribution that argues against "thickness" as a major contributor to values of σ'. Four benzenes that are di-substituted in the *para* position were found to have consistently lower values of σ', by an average of -0.26 ± 0.04 units. Two benzenes substituted by bulky tertiary substituents were found to have higher than expected values of σ', by $+0.26 \pm 0.03$ units. These various deviations from Eq. (4) in Table 3 might represent either "real" contributions of molecular structure to σ', or systematic errors in the representation of molecular length L by the present convention (Section 2.2.3). Finally, it was shown previously [27] that solute planarity (e.g., biphenyls substituted in the 2-position) plays a very minor role in affecting values of σ'.

4.1.2. Values of η' as a function of solute molecular structure

Values of η' are highly correlated with solute retention ($\log k$) [11], which has in turn been exhaustively studied as a function of solute molecular structure (e.g., [34]).

4.2. Values of H and S* as a function of column properties

While steric interaction and values of S^* are of primary interest, it will prove useful to compare values of both H and S^* in terms of their dependence on ligand length n, pore diameter d_{pore}, ligand concentration C_L, and end-capping – as described by Eq. (3). The dependence of H on column properties is examined in Section 4.2.1, followed by a similar look at S^* in Section 4.2.2. Steric interaction and shape selectivity are then compared in Section 4.3.

Table 4
Summary of regression of column parameters vs. properties (Eq. (3)).

	H	S^*
Number of omitted columns	24	11
r^2	0.9274	0.775
std. error SE	0.0314	0.019
a (intercept)	0.5285	−0.165
b (ligand length n)	0.0422	0.009
c (n^2)	−0.0010	−0.0003
d (pore diameter d_{pore})	−0.0110	−0.002
e (d_{pore}^2)	0.0002	0.0000
f (bonding concentration C_L)	0.0444	0.031
g (C_L^2)	−0.0032	−0.002
h (end capping)	0.0332	0.067

4.2.1. Column hydrophobicity H

The application of Eq. (3) to the 167 type-B alkylsilica columns resulted in an initial correlation for H of $r^2 = 0.777$, but with outliers that deviated by 2.6 or more times the standard error of the correlation for all columns. The latter, deviating columns were successively deleted from the regression, until $r^2 = 0.927$ for the remaining 143 columns. The rejected outliers are believed to be the result of additional contributions to H that are unreported by the manufacturer: differences in (a) the silane used to bond the column, (b) the starting silica and its relative hydration, and (c) other changes in the chemistry of the manufacturing process. A more detailed justification of our deletion of outliers is offered in Appendix A. A summary of the latter regression is shown in Table 4 for the column parameter H. For these 143 columns, we see that about 93% of the total variance in values of H has been accounted for by four properties of the column (n, d_{pore}, C_L, and end-capping). Most of the remaining 7% variance (as well as the above 24 column-outliers) appears to arise from differences in the silica used to prepare the column packing, as well as other changes in the manufacturing process that might affect solute retention [35–38] – *apart* from their effect on pore diameter or ligand concentration. See the further analysis of Appendix A which supports this conclusion.

Column hydrophobicity H is the primary factor that determines RPC retention. Fig. 11 illustrates the dependence of H on ligand length n (a), pore diameter d_{pore} (b), ligand concentration C_L (c), and end-capping (d) – as predicted by Eq. (3) and Table 3 (closed circles). The two dashed curves for each plot in Fig. 11a–c provide an estimate of reliability or error; each of the latter plots results from the separate regressions of two randomized column subsets that comprise 71 and 72 of the original 143 columns (after deletion of outliers). In Fig. 11a–c the values of other column properties from Eq. (3) are assumed equal to their average values for all 167 columns (values noted in the figure), and the predicted values of Fig. 11a–c also assume end-capped columns. The vertical scale for Fig. 11a–d is in each case the same, allowing a visual comparison of the relative effect of each column property on H. Comparable plots are obtained from regressions as in Table 4 when no outliers are deleted, and similar conclusions regarding H as a function of column properties therefore result.

For $n \leq 22$, values of H increase with ligand length (Fig. 11a), then decrease slightly as n increases further. An increase in pore diameter d_{pore} leads to a decrease in H. Values of H increase for greater ligand concentration, with a gradually decreasing effect as C_L increases. Finally, end-capping (Fig. 11d) adds 0.033 units to H – a relatively minor increment. The contribution of each column property to H likely affects contributions from other column properties, but the introduction of combined terms (e.g. nd_{pore}) into Eq. (3) did not improve the correlation significantly.

Larger values of H imply increased contact between column ligands and the retained solute. An increase in H with increased ligand concentration is therefore expected (Fig. 11c). Likewise, a decrease

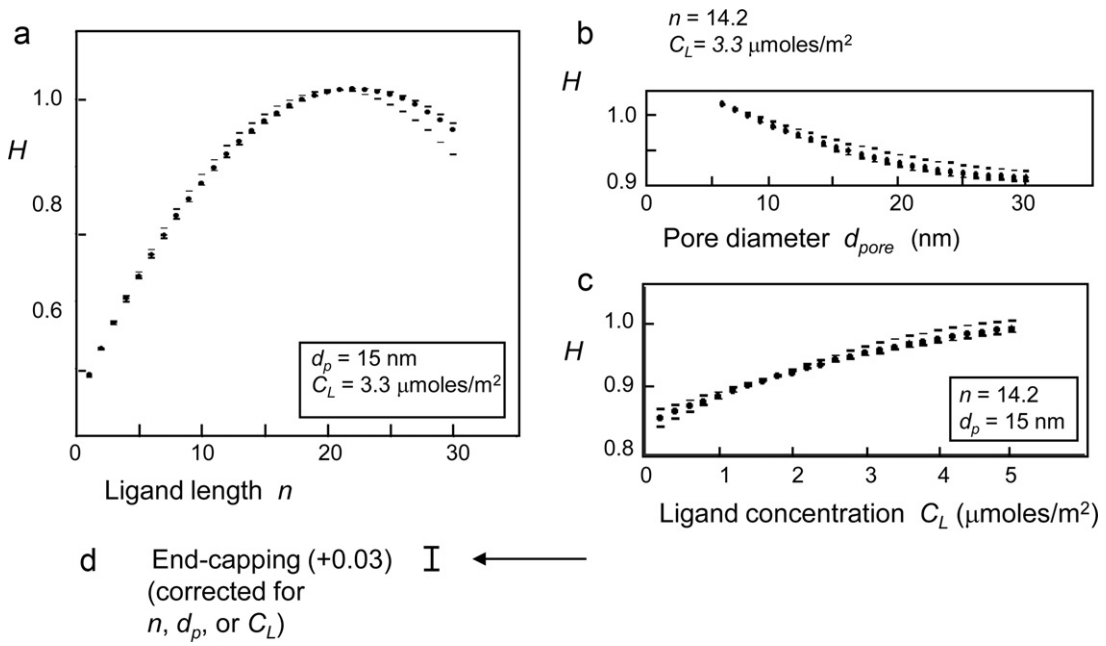

Fig. 11. Dependence of H on column properties; plots created from coefficients of Table 4. (– – –) uncertainty limits; see text for details.

in pore diameter with corresponding increase in the curvature of the pore (assuming cylindrical pores) will lead to increased crowding of the ligand ends, again with an increase in solute–ligand contacts and H (Fig. 11b). An increase in H with ligand length (Fig. 11a) is expected, due to the resulting increased probability of solute–ligand contacts.

4.2.2. Column steric interaction S^*

The application of Eq. (3) (with S^* replacing H) to the original 167 type-B alkylsilica columns resulted in an initial correlation of $r^2 = 0.577$, but with outliers that deviated by 2.6 or more standard deviations. The latter columns were successively deleted from the regression, until $r^2 = 0.775$ for the remaining 156 columns. A summary of this regression is shown in Table 4 for the column parameter S^*. For the latter 156 columns, we see that about 77% of the total variance of values of S^* has been accounted for. As for values of H, most of the remaining 23% variance appears to arise from differences in silica and the column-packing manufacturing process (see Appendix A).

Fig. 12 illustrates the dependence of S^* on ligand length n (a), pore diameter d_{pore} (b), ligand concentration C_L (c), and end-capping (d) – with other column properties held constant at the same average values indicated in Fig. 11a–c for each corresponding plot. The columns of Fig. 12a–c are assumed to be end-capped, and the dashed curves again represent an estimate of the uncertainty in each plot. As in the case of Fig. 11, the vertical scale for each of Fig. 12a–d is the same (but much expanded vs. that of Fig. 11), allowing a visual comparison of the relative effect of each column property on S^*.

S^* increases with ligand length for small values of n, reaches a maximum value for $n \approx 15$, then undergoes a steep decrease for larger values of n (Fig. 12a). Since the value of S^* is similar for both C_1 and C_{30} columns, and there can be little steric interaction for a C_1 column, it appears that there is likewise a near-zero contribution of steric interaction for C_{30} columns. Values of S^* decrease with increasing pore diameter, and approach a limiting value for $d_{pore} \approx 30$ nm (Fig. 12b). Ligand concentration has the largest effect on S^* (Fig. 12c), which increases steadily as C_L increases. End-capping (Fig. 12d) increases values of S^* by 0.067 units, an effect that is larger than that of either ligand length or pore diameter, and is relatively much greater than the effect of end-capping on H.

The effects of column properties on S^* can be compared with the similar dependencies for H. S^* and H both increase initially for an increase in n or C_L. In each case, the effects of pore diameter are relatively small, and can be rationalized by the increase in ligand crowding for smaller pore diameters. The effect of ligand concentration C_L is relatively much larger for S^*, as expected; that is, as C_L increases, the space between ligands decreases, in turn reducing the volume available for the free movement of a retained solute. The dependence of S^* on ligand length n is surprising, with one interpretation offered in Section 4.4.2.

The much larger relative effect of end-capping on values of S^* vs. H is striking, since end-capping would appear to have little direct effect on ligand crowding or conformation. The relatively large effect of end-capping on S^* (+0.067 from the regression of Table 4) is supported by the data of Fig. 13, where the distribution of S^*-values for end-capped (a) and non-end-capped columns (b) are compared. The dashed lines in Fig. 13a indicate the average value of S^* for non-end-capped columns (±1 SD) from Fig. 13b. There is a *difference* in average values of S^* of +0.083 for end-capped vs. non-end-capped columns. A direct measurement of the effect of end-capping was provided by values of S^* for a Symmetry C18 stationary phase that was prepared with and without end-capping [27]; S^* for the end-capped column was higher by +0.03 units (only half as large as the above values, but still significant). End-capping reduces the amount of water and organic solvent held near the substrate surface of the stationary phase [39], which in turn limits ligand flexibility [28]. The result should be an increase in S^*, as observed.

4.2.2.1. Values of S^* for other column types. Values of S^* for several cyano and phenyl columns have also been measured. Table 5 compares average values of S^* for the latter column types with values for alkylsilica columns of similar ligand length n; no attempt was made to correct for differences in ligand concentration, pore diameter, or end-capping (note that the length of a phenyl group is about the same as that of a C_4 group). The difference in values of S^* for each column type of Table 5 and S^* for the corresponding alkylsilica column (i.e., for comparable ligand length) is shown in the last data column of Table 5. It is seen that cyano and phenyl columns

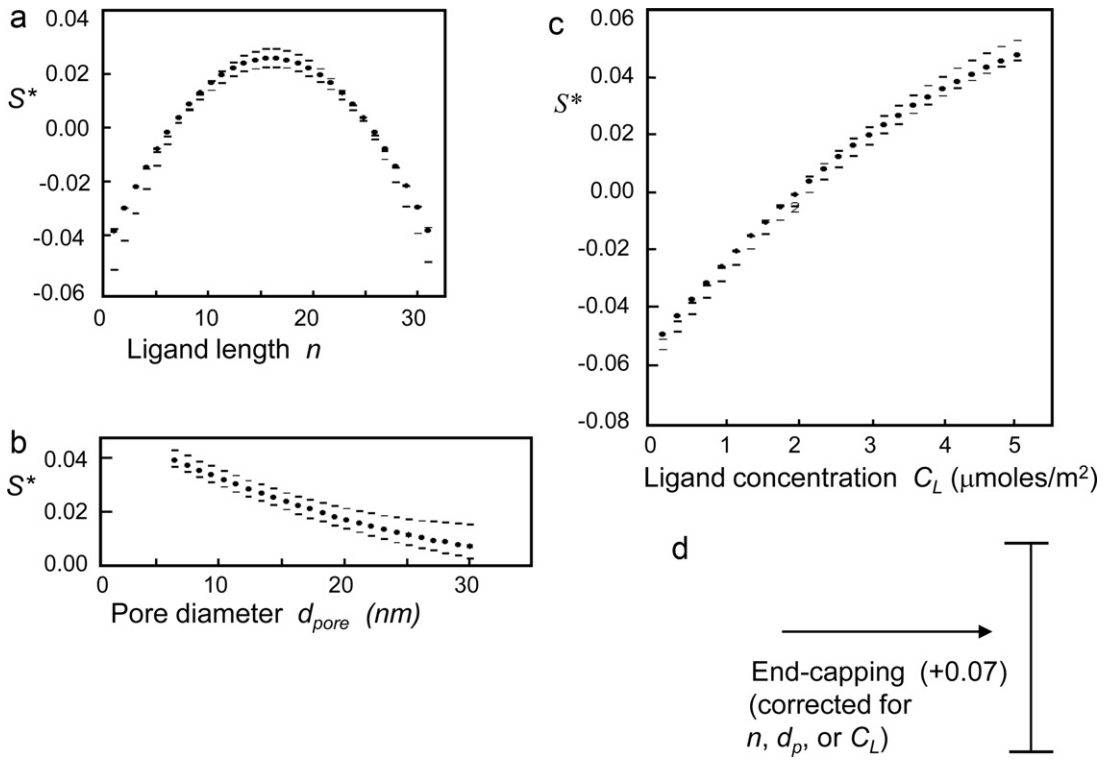

Fig. 12. Dependence of S^* on column properties, (– – –) as in Fig. 11 for H.

exhibit less steric interaction than alkylsilica columns of similar ligand length. Siepmann has noted [29] in this connection that ligand conformational entropy will be less for more rigid ligands such as phenyl and cyano, and values of S^* should therefore be less (as observed). However, poorer accuracy is observed for the application of Eq. (2) to columns other than type-B alkylsilica [11], a factor that may introduce error into values of S^* for such columns.

Euerby has reported a rather large shape selectivity for PFP columns, based on the relative retention of triphenylene vs. *o*-terphenyl ($\alpha_{T/O}$) [40]. However, all the columns of Table 5 are capable of π–π interaction with aromatic solutes [41–43], while values of $\alpha_{T/O}$ are derived from the retention of two solutes whose tendency for π–π interactions is expected to be significantly different. This would in turn lead to values of $\alpha_{T/O}$ for phenyl or cyano columns that as measures of shape selectivity are likely to be somewhat compromised. It should also be noted that the correlation of values of $\log(\alpha_{T/O})$ and S^* is poor ($\log[\alpha_{T/O}] = -0.12 - 0.85S^*$; $r^2 = 0.27$), although in the expected direction (based on values of $\alpha_{T/O}$ for 51 type-B alkylsilica columns for which values of S^* are available [24]). For a further discussion of shape selectivity with phenyl columns, see [44].

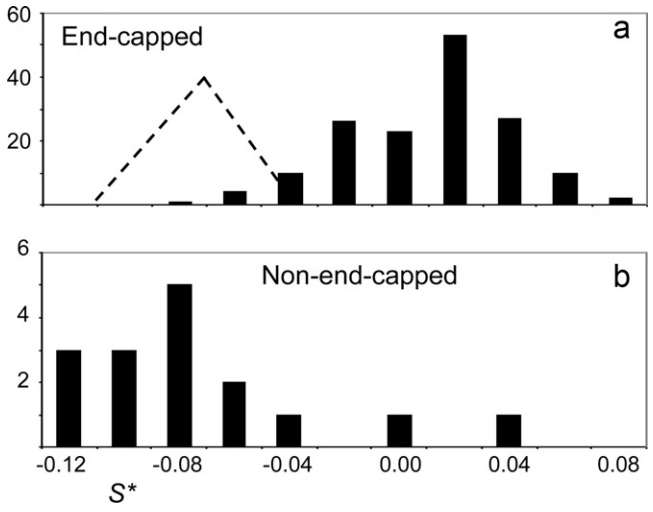

Fig. 13. Distribution of values of S^* for end-capped columns (a) and non-end-capped columns (b). See text for details.

4.3. Comparison of steric interaction S^* with shape selectivity Φ_{SS} in terms of column properties and temperature

While the lack of correlation of values of S^* and Φ_{SS} suggests that steric interaction and shape selectivity represent two different processes, further supporting evidence for this conclusion is summarized in the present section. Note, however, that the H-S model and Eq. (2) are based mainly on monomeric columns at 35 °C, while shape selectivity is most pronounced for polymeric columns and/or lower temperatures. Consequently the following comparisons of shape selectivity with steric interaction in many cases involve different separation conditions.

4.3.1. Ligand length

The data of Figs. 5a and 12a for monomeric columns are compared in Fig. 14. Absolute values of S^* and Φ_{SS} are not directly comparable, but both steric interaction and shape selectivity are expected to be negligible for a C_1 column. The curve in Fig. 14 for

Table 5
Values of S^* for other column types [41,42].

Column	S^* (avg)	std. dev.	L	S^* (alkylsilica)	S^*–S^* (alkylsilica)
Perfluorophenyl (PFP)	−0.114	0.036	8	−0.000	−0.114
Phenyl	−0.13	0.068	7	−0.004	−0.134
Cyano	−0.139	0.037	5	−0.019	−0.12
Phenyl hexyl	−0.085	0.046	10	0.008	−0.077

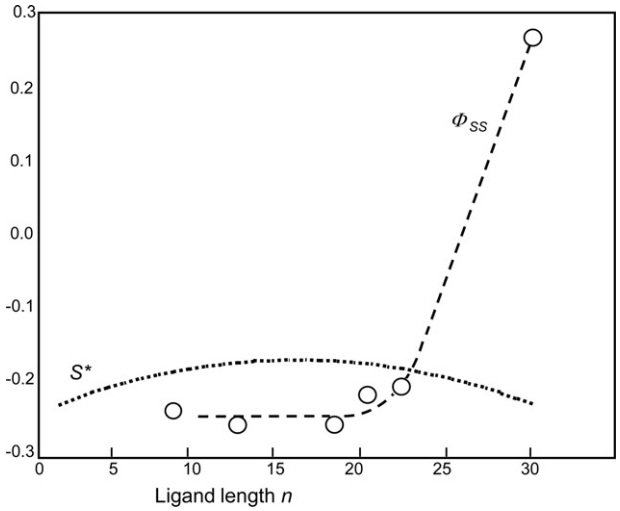

Fig. 14. Comparison of steric interaction S^* and shape selectivity Φ_{SS} for monomeric alkylsilica columns as functions of ligand length n. Data from Figs. 5a and 12a.

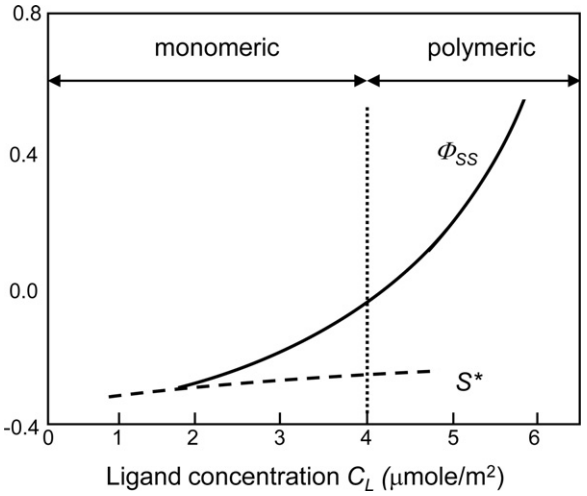

Fig. 15. Comparison of steric interaction S^* and shape selectivity Φ_{SS} as functions of ligand concentration C_L. Data of Figs. 5c and 12c.

S^* has therefore been transposed vertically so as to coincide with the curve for Φ_{SS} at C_1. From Fig. 14 we see that the dependence of steric interaction and shape selectivity on n is quite different, with shape selectivity being much more significant for C_{30} columns. Our present picture of shape selectivity features either solute exclusion or a need to create cavities in the stationary phase for solute insertion; steric interaction, on the other hand, seems to emphasize a loss of freedom of the solute within the stationary phase (but note the further discussion of Section 4.4.2). For values of $n > 20$, exclusion and/or cavity formation begin to predominate, with a transition from steric interaction to shape selectivity as the dominant process.

4.3.2. Ligand concentration

The relative effects of ligand concentration C_L on values of S^* and Φ_{SS} are compared in Fig. 15 for C_{18} columns (data of Figs. 5c and 12c). Both steric interaction and shape selectivity increase with ligand concentration, but shape selectivity becomes progressively more affected by ligand concentration for values of $C_L > 4$. Figs. 5c and 12c suggest that steric interaction and shape selectivity coexist to some degree for the monomeric columns of the present study.

4.3.3. Pore diameter

It has been reported that shape selectivity is greater for wide-pore columns [45], which is the opposite of steric interaction (Fig. 12b).

4.3.4. End-capping

There is no effect of end-capping on shape selectivity [45], but end-capping has a relatively large effect on steric interaction (Fig. 12d, monomeric columns).

4.3.5. Temperature

As seen in Fig. 5b, an increase in temperature from 35 °C to 45 °C results in a slight decrease in shape selectivity for a monomeric column, but a larger decrease for a polymeric column. For either column type, this suggests an inherently enthalpic nature for shape selectivity. In the case of a (monomeric) Symmetry C18 column, for which we can calculate a change in S^* from data reported in [46], its value of $S^* = 0.063$ is relatively high (average value for all columns of Table 2 is $S^* = 0.002 \pm 0.040$ [1 SD]), indicating greater-than-average steric interaction for this column. A 10 °C increase in temperature changes the value of S^* for this column by +0.002 units – a negligible amount and in opposite direction to the effect of temperature on shape selectivity. The latter lack of a temperature dependence for S^* appears consistent with the model of Fig. 7, which implies that steric interaction is controlled primarily by entropy rather than enthalpy.

4.4. The nature of steric interaction

Various results discussed above can now be further interpreted to arrive at an enhanced description of steric interaction.

4.4.1. Differing natures of steric interaction S^* and shape selectivity Φ_{SS}

The comparisons of Section 4.3 suggest that these two examples of steric hindrance in the stationary phase represent significantly different retention processes. While shape selectivity has received considerable attention over the past two decades [12–16], our present understanding of steric interaction is more limited. This is partly due to the much smaller contribution of steric interaction to retention (compared to shape selectivity), as well as the complex nature of a purely entropic process (like SEC) that is at the same time affected by accompanying enthalpic (hydrophobic and other) contributions to overall solute retention. While it seems clear that steric interaction is not the same as shape selectivity, the evidence in favor of the model of Fig. 7 for steric interaction might be regarded as still incomplete. It should also be kept in mind that our data are based on monomeric columns at 35 °C, conditions for which shape selectivity exerts a minimal effect on retention.

Because shape selectivity represents a solute–column interaction not included in Eq. (2) (just as for π–π and dipole–dipole interactions mentioned in Section 4.2.2.1), the extension of Eq. (2) for solutes and columns that exhibit significant shape selectivity would require the addition of an additional (sixth) term.

4.4.2. Stationary-phase structure and its consequences

Perhaps the most striking feature of Fig. 12 is the dependence of S^* on ligand length n, where a maximum in S^* for $n \approx 15$ is observed. We believe that this behavior can be rationalized as follows. A rough approximation to the configuration of a series of stationary phases comprising ligands of different lengths n is shown by the cartoons of Fig. 16a. As n increases from C_1 to C_{18}, there is increased ligand flexibility and folding–but little entanglement of one ligand with another [39]. Monte Carlo simulations [47] further suggest that solutes are retained on the top (exterior) of a C_1 column

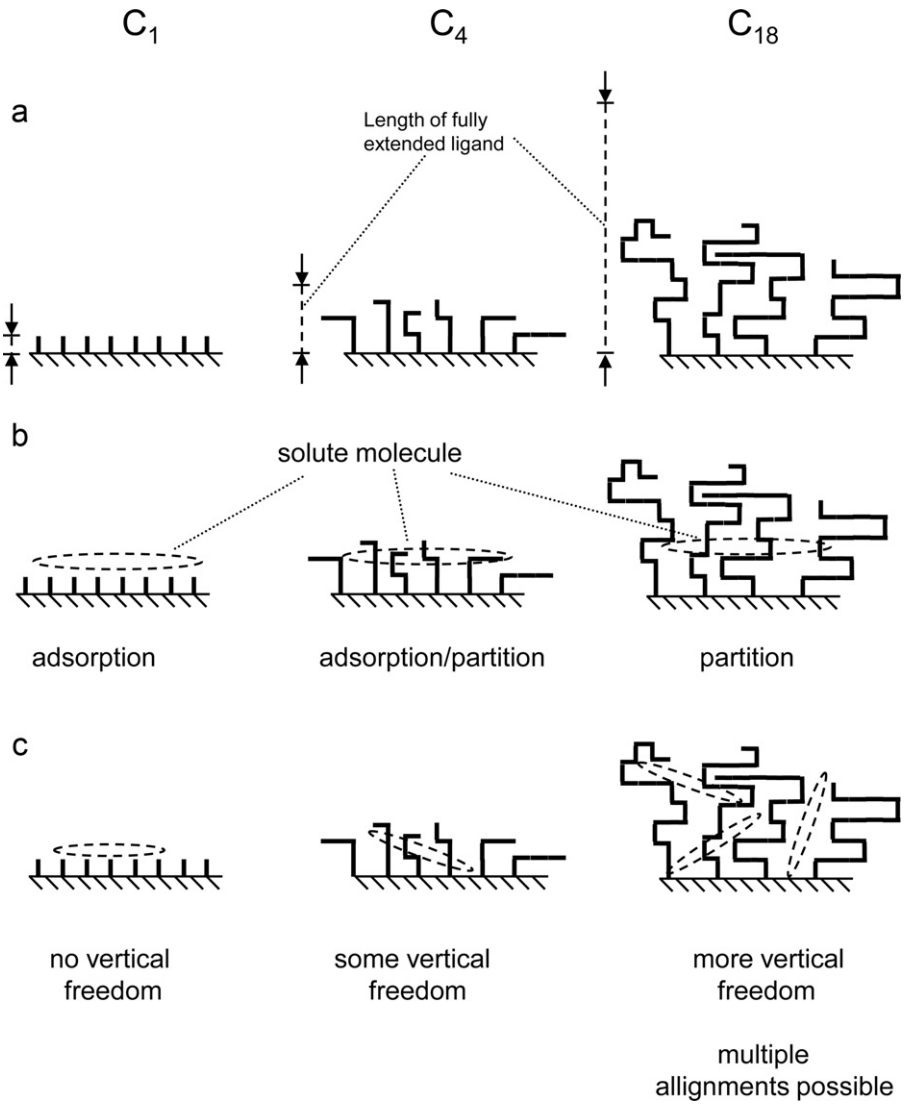

Fig. 16. Cartoon representations of the stationary phase for ligands of different length, with their possible effects on steric interaction. (a) Ligand configuration vs. ligand length; (b) adsorption vs. partition for ligands of different length; (c) freedom of movement of solute molecule as a function of ligand length. See text for details.

(adsorption), in an intermediate position (adsorption/partition) for a C_4 column, and with greater penetration into the interior region of the bonded phase of a C_{18} column (partition) – as in Fig. 16b. With increasing penetration into the stationary phase, the solute molecule is increasingly constrained, with its entropy of retention becoming less favorable; this results in some steric exclusion and an increase in S^*. However, with increasing ligand length, new orientations of the solute become possible (Fig. 16c), which still permit intimate contact between nonpolar solutes and the ligand chain. There is also increasing vertical space in which the solute can align itself with ligands that are long enough (e.g., C_{18} in this example).

We therefore see two opposing contributions to steric exclusion (and steric interaction) as n increases. First, for larger n and increasing partitioning into the stationary phase, S^* will increase – but as n becomes large enough, there is a countervailing tendency due to the increased space within the stationary phase – potentially resulting in a reversal of values of S^* as a function of n (as in Fig. 12a). Finally, longer ligands offer increased opportunities for the formation of cavities into which bulky molecules can enter, because longer ligands can more easily bend to create spaces into which a solute is inserted. The result of these various contributions to S^* is as observed in Fig. 12a: a maximum value of S^* for an intermediate ligand length. *Thus as ligand length increases further from C_{18} to C_{30}, solute partitioning becomes complete (i.e., constant), while inter-ligand space increases and cavity formation becomes easier*. These various contributions to values of S^* could reasonably lead to a steep decline in S^* for C_{30} vs. C_{18} as in Fig. 12a.

It might be argued that an increase in solute molecular volume V, with a consequent requirement for a larger containment space within the stationary phase, represents an alternative description of steric interaction. There is no hard evidence to distinguish the two possibilities. For 87 solutes (Table 4 of [10]), values of σ' were regressed vs. either L, L^2 ($r^2 = 0.530$) or V, V^2 ($r^2 = 0.402$). This result tends to support a somewhat larger role for L vs. V.

A purely entropic explanation for steric interaction is complicated by the associated (enthalpic) retention of the solute, as well as by possible localization effects noted in Section 4.1. It should also be noted that the solute molecules for which we have values of σ' are generally shorter than a C_{18} ligand. When $L > n$, the situation likely becomes more complicated.

5. Conclusions

Conclusions from the present study derive from (a) the "bulkiness" of solute molecules (σ') as a function of molecular

structure, (b) the resistance to penetration of the stationary phase (S^*) vs. column properties, and (c) comparisons of values of S^* (steric interaction) with values of Φ_{SS} (shape selectivity). While steric interaction represents a relatively minor contribution to column selectivity, its further investigation here can be justified by its importance to the application of the hydrophobic-subtraction model – of which steric interaction forms an essential part.

It has previously been established that values of σ' correlate approximately with solute molecular length L. A more accurate relationship between σ' and L was established by restricting the correlation to 28 solutes that should be largely free from solute–column interactions other than hydrophobic or steric (Eq. (4) and Fig. 9 for which $r^2 = 0.87$). When experimental values of σ' for other solutes were compared with Eq. (4), a similar agreement was found for 11 benzenes substituted by polar groups and 23 *n*-alkanes substituted in the 1-position by a single polar group (*in toto*, 41% of the 150 solutes for which we have values of σ'). This strongly supports solute molecular size as the main contributor to steric interaction.

Values of σ' for 33 other solutes exhibit sizable negative deviations vs. values from Eq. (4) (Fig. 10c–f). Each of these deviating solutes is capable of strong hydrogen-bonding or electrostatic interactions with the stationary phase, resulting in partial localization of the molecule, and a consequent reduction in values of σ'. Values of σ' for the remaining 49 solutes (more complex molecules of varied structure) followed a similar pattern: 16 of these solutes exhibited significant (generally negative) deviations from Eq. (4) and in most cases are capable of strong interactions with the stationary phase.

Values of S^* and column hydrophobicity H for 167 type-B alkylsilica columns (Table 2) were regressed vs. various column properties: ligand length and concentration, pore diameter, and whether the columns are end-capped. With deletion of 11–24 outliers, resulting correlations gave r^2 values of 0.93 for H and 0.78 for S^*. Remaining contributions to variance (and the greater errors found for deleted columns) are believed due to differences in the silica and manufacturing process for various columns, on the basis of data for "matched" C_8 and C_{18} columns (see Appendix). Column hydrophobicity H and steric interaction S^* might each be expected to increase with ligand length and ligand concentration, decrease with pore diameter, and be little affected by end-capping. This is generally true for values of H, but with some important differences. Thus, H tends to increase with ligand length n initially, then level off for $n > 20$, while S^* goes through a distinct maximum for $n \approx 15$. The latter behavior is believed to arise as follows. For short ligands (small values of n), molecular simulations show that the retained molecule is adsorbed on top of the stationary phase. As n increases, adsorption changes to partition, with increased constraint of the retained solute (increased steric interaction and resulting larger values of S^*). At the same time, an increase in n corresponds to an expanded inter-ligand space with reduced constraint of the solute molecule. It is proposed that increased partitioning determines values of S^* for $n < 15$, while for $n > 15$ a further increase in inter-ligand space (plus easier formation of cavities for the solute molecule) becomes progressively more important. Finally, for $n = 30$, there appears to be a near absence of steric interaction (and a transition from steric interaction to shape selectivity for monomeric columns).

End-capping increases values of H only slightly, but increases S^* by a relatively large amount. While the reason for this is still unclear, one possibility is that end-capping reduces the amount of entrained mobile phase near the silica surface, which in turn reduces ligand flexibility.

Comparisons of steric interaction (values of S^*) with shape selectivity (Φ_{SS}) show several differences:

- long vs. wide molecules of similar molecular weight preferentially retained by shape selectivity, but less retained by steric interaction
- nonplanar molecules less retained by shape selectivity; little difference for steric interaction
- no correlation of values of S^* and Φ_{SS}
- opposite effects of end-capping, pore diameter, or temperature on S^* and Φ_{SS}
- very different effects of ligand length

While both of these phenomena reflect steric hindrance in the stationary phase, steric interaction appears to be more the result of a decrease in entropy for retained "bulky" molecules, while shape selectivity more closely resembles an enthalpic process that requires the presence or creation of spaces within the stationary phase for retained solute molecules. Steric interaction can also be described as arising from a decrease in entropy as a result of a decreased number of available solute conformations/positions within the stationary phase. Shape selectivity seems to involve a more drastic rearrangement of the stationary phase in order to allow entry of the solute.

Steric hindrance in the stationary phase is a complex phenomenon whose details depend on the nature of the column, the molecular size and shape of an individual solute, and other separation conditions. While some aspects of steric interaction have been brought into better focus in the present study, further work on shape selectivity and especially steric interaction should contribute to a more complete picture.

Nomenclature

A	column hydrogen-bond acidity
B	column hydrogen-bond basicity
C	column cation-exchange capacity
C_L	stationary-phase ligand concentration (μmole/m^2)
d_{pore}	particle pore diameter (nm)
E_C	end-capping; $E_C = 1$ for end-capped columns, 0 for non-end-capped columns
H	column hydrophobicity
H-B	hydrogen-bond
H-S	hydrophobic-subtraction
k	retention factor
k_{BaP}	value of k for benzo[a]pyrene
k_{EB}	value of k for ethylbenzene
k_{TBN}	value of k for tetrabenzonaphthalene
L	solute molecular length (Section 2.2.3)
L/B	length-to-breadth ratio of a molecule
n	stationary-phase ligand length; e.g., $n = 18$ for a C18 column
PFP	pentafluorophenyl (column)
r^2	coefficient of determination
RPC	reversed-phase chromatography
S^*	steric resistance to insertion of bulky solute molecules into the stationary phase
t_R	retention time (min)
t_0	column dead-time (min)
V	solute molar volume (mL)

Greek letters

α	selectivity; k_2/k_1 for two peaks 1 and 2
α'	solute hydrogen-bond acidity
$\alpha_{TBN/BaP}$	equal to k_{TBN}/k_{BaP}
$\alpha_{T/O}$	equal to k for triphenylene divided by k for *o*-terphenyl
β'	solute hydrogen-bond basicity

$\delta \log k$	difference between experimental and calculated values of k from Eq. (1); see Fig. 1
Φ_{SS}	$\log(1/\alpha_{TBN/BaP})$; a measure of shape selectivity comparable to S^* for steric interaction
δH	error in predicted value of H from Eq. (3); see Appendix A
δS^*	error in predicted value of δS^* from Eq. (3); see Appendix A
$\delta\sigma'$	a contribution to values of σ' other than solute molecular length; experimental value of σ' minus value from Eq. (4)
η'	solute hydrophobicity
κ'	charge on solute molecule (positive for cations, negative for anions)
σ'	steric resistance of solute molecule to penetration into stationary phase

Acknowledgements

Experimental measurements of column selectivity parameters (Table 2) were carried out by Nan Wilson, Jonathan Gilroy, and Chris Heard (BASi Northwest Laboratory, McMinnville, OR). We are also grateful for the helpful comments of Drs. Lane Sander (NIST) and Ilja Siepmann (Univ. Minnesota), while recognizing that full agreement on every detail of this complicated story has yet to be achieved.

Dr. Uwe Neue, one of the authors of the present paper, had been an active participant in the development of the hydrophobic-subtraction model from the first planning session in 1998. Over the subsequent years he supported this project in numerous ways, and his well-known experience and competence in the area of HPLC column technology were of prime importance. Unfortunately his active and promising life was cut short in late 2010. We will all miss him.

Appendix A. Contributions to H and S^* other than known column properties

Apart from varying column properties (n, d_{pore}, C_L, end-capping), the final stationary phase (and values of H or S^*) may differ further as a result of various changes in the manufacturing process [35–38], including the use of different silanes, silicas, or reaction conditions for the bonding process. Such (usually proprietary) differences could be responsible for the failure of Eq. (3) to fully account for the variance in values of H or S^*. Columns whose value of H or S^* are markedly affected by column characteristics other than n, d_{pore}, C_L, end-capping would in turn lead to error in resulting coefficients a–h from Eq. (3). For this reason, we have chosen to exclude columns with absolute deviations δH or δS^* (vs. values predicted by Eq. (3)) that are greater than 2.6 times the standard error SE: #3, 4, 13, 14, 15, 23, 40, 50, 64, 71, 81, 82, 99, 107, 108, 115, 116, 120, 122, 136, 137, 144, 146, and 155 (H) and #3, 13, 14, 17, 20, 39, 56, 76, 99, 107, 163 (S^*) of Table 2.

This deletion of outliers can be justified on various grounds. For the 167 columns under consideration, the probability of an absolute error greater than 2.6 SE is only 0.004, corresponding to 1.3 columns out of 167; this can be compared with 24 columns with values of δH this large, and 11 columns with corresponding values of δS. In this connection, it is useful to examine the distribution of values of δH and δS shown in Fig. 17a and b. Values of δH or δS^* equal to ± 2.6 SE are indicated by arrows in each figure. It is seen that absolute values of δH or δS^* outside the latter limits (arrows) are in most cases $\gg 2.6$ SE, further justifying their exclusion in the application of Eq. (3).

The fit of Eq. (3) based on excluded columns has been compared with corresponding fits of separate column sub-sets (dashed curves of Figs. 10 and 11). Their close agreement with the fit for all but excluded columns is quite good, supporting the reliability of the results of Table 4 based on excluded columns. A similar validation of the data of Table 4 is provided by column pairs that are expected to differ to a lesser degree in both starting materials and manufacturing detail. See following Sections A.1 and A.2.

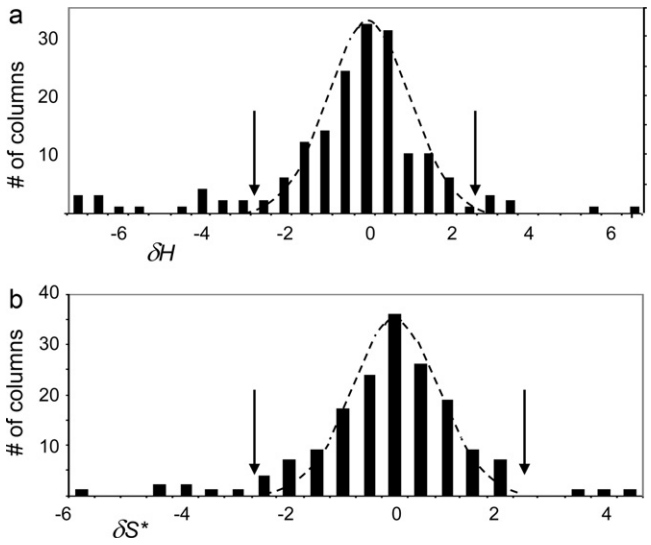

Fig. 17. Distribution of errors in values of H (a) and S^* (b) predicted by Eq. (3). See Appendix A for details.

A.1. Column hydrophobicity H

If we consider matched columns that differ only in the ligand – for example, Symmetry C18 vs. Symmetry C8 – the use of the same silica and a similar manufacturing process seems likely for many (but not necessarily all) such matched column-pairs. It will prove convenient to discuss the effect of these added contributions to H in terms of the quantity δH, equal to the experimental value of H minus the value calculated from Eq. (3) (i.e., the error in calculated values of H). We might expect similar values of δH for each of two such matched columns, as any contribution to H beyond that from the variables of Eq. (3) is expected to be similar for matched columns (assuming the same silica and similar manufacturing conditions). There are 30 pairs of matched columns among the 167 columns under study, for each of which pairs we can determine the standard error SD for their δH values (#1, 2; 6, 10; 12, 15; 21, 22; 23, 24; 37, 38; 50, 52; 53, 54; 55, 57; 59, 60; 62, 63; 65, 67; 70, 72; 73, 75; 76, 77; 84, 86; 87, 90; 98, 99; 103, 104; 122, 123; 124, 126; 129, 130; 133, 137; 148, 149; 153, 154; 155, 156; 157, 158; 160, 161; 162, 164; 165, 167). In the absence of any unusual similarity of a C_8 vs. a C_{18} column, the std. deviation of values of δH for two matched columns (SD[δH]) should (on average) equal $2^{1/2}$ times the SD value of Table 4; i.e., $2^{1/2} \times 0.0314 = 0.0444$. If certain contributions to H other than those predicted by Eq. (3) are similar for matched columns, actual values of SD(δH) for these columns should be generally smaller than 0.0444. This prediction is tested in Fig. 18a, as a frequency plot of values of SD(δH) for matched columns. As expected, the majority of column-pairs (25) have SD(δH) < 0.044 (arrow).

Inasmuch as manufacturing conditions may occasionally be quite different for some of these column-pairs, values of SD(δH) > 0.044 in Fig. 18a are also not unexpected. A cluster of three such outliers is seen in Fig. 18a, with SD > 0.044. Presumably these column pairs *have* experienced greater differences in their preparation. With the exclusion of these three outliers, the average value of SD for the remaining 27 column pairs is only 0.014, corresponding to an unaccounted for variance in H of just 1% (as compared with 7% if differences in column manufacture are ignored).

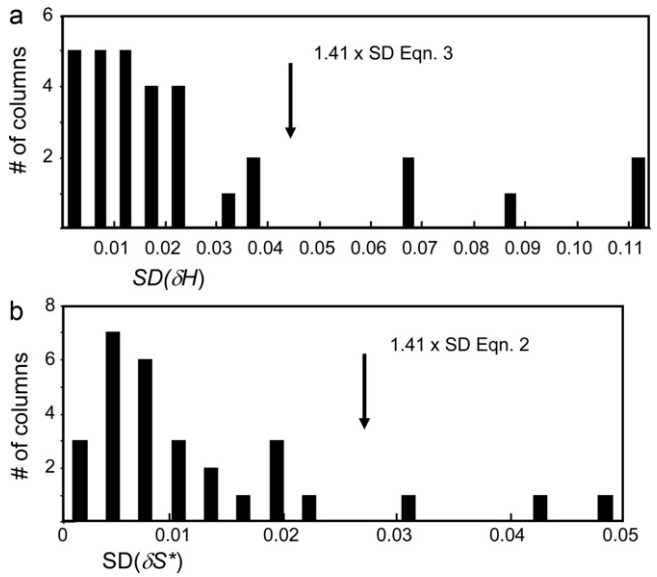

Fig. 18. Origin of unexplained contributions (δH and δS^*) to H (a) and S^* (b) as shown by "matched" C_8 and C_{18} columns. See Appendix A for details.

A.2. Steric interaction S^*

As in the case of values of H, we expect similar values of δS^* (error in Eq. (3)) for each of two matched columns (e.g., Discovery C_{18} and C_8). We also expect that the std. deviation of values of δS^* (SD[δS^*]) for different column pairs will tend to be smaller than $2^{1/2}$ times the std. error (SE = 0.019) for the 159 columns used with Eq. (3) ($2^{1/2} \times 0.019 = 0.027$). Fig. 18b provides a frequency distribution of values of SD for the 30 matched column-pairs; the majority of column-pairs (27) are indeed seen to have SD(δS^*) < 0.027 (arrow). Three outliers in Fig. 18b have SD > 0.027. With the exclusion of these outliers, the average value of SD for the remaining 27 column pairs is 0.007, corresponding to a residual variance of only 3% (as compared with 23% if differences in column manufacture are ignored). The generally small values of SD(δS^*) for matched columns also represents a further check on the validity of Eq. (3) and the accuracy of measurement of values of S^*.

Finally, "matched" columns that give larger errors in H from Eq. (3) might be expected to give larger errors in S^*, although an exact correspondence is not expected. Later studies will extend the analysis of "matched" columns to the remaining column parameters A, B and C. Preliminary results do show a tendency for certain columns to give larger errors for these various column parameters.

References

[1] A. Tchapla, H. Colin, G. Guiochon, Anal. Chem. 56 (1984) 621.
[2] L.C. Tan, P.W. Carr, J. Chromatogr. A 775 (1997) 1.
[3] A. Ailaya, Cs. Horváth, J. Chromatogr. A 829 (1998) 1.
[4] S.C. Rutan, J.M. Harris, J. Chromatogr. A 656 (1993) 197.
[5] R.K. Gilpin, J. Chromatogr. A 656 (1993) 217.
[6] K.B. Sentell, J. Chromatogr. A 656 (1993) 231.
[7] H.J. Egelhaaf, D. Oelkrug, M. Pursch, K. Albert, J. Fluorescence 7 (1997) 311.
[8] B. Buszewski, S. Kowalska, K. Krupczyńska, Crit. Rev. Anal. Chem. 35 (2005) 89.
[9] J.L. Rafferty, J.I. Siepmann, M.R. Schure, J. Chromatogr. A 1216 (2009) 2310.
[10] N.S. Wilson, M.D. Nelson, J.W. Dolan, L.R. Snyder, R.G. Wolcott, P.W. Carr, J. Chromatogr. A 961 (2002) 171.
[11] L.R. Snyder, J.W. Dolan, P.W. Carr, J. Chromatogr. A 1060 (2004) 77.
[12] L.C. Sander, S.A. Wise, J. Chromatogr. A 656 (1993) 335.
[13] L.C. Sander, S.A. Wise, Anal. Chem. 59 (1987) 2309.
[14] L.C. Sander, M. Pursch, S.A. Wise, Anal. Chem. 71 (1999) 4821.
[15] L.C. Sander, K.A. Lippa, S.A. Wise, Anal. Bioanal. Chem. 382 (2005) 646.
[16] C.A. Rimmer, K.A. Lippa, L.C. Sander, R.E. Majors, LC-GC North Am. 26 (2008) 984.
[17] J.W. Dolan, A. Maule, D. Bingley, L. Wrisley, C.C. Chan, M. Angod, C. Lunte, R. Krisko, J.M. Winston, B. Homeier, D.V. McCalley, L.R. Snyder, J. Chromatogr. A 1057 (2004) 59.
[18] J. Pellett, P. Lukulay, Y. Mao, W. Bowen, R. Reed, M. Ma, R.C. Munger, J.W. Dolan, L. Wrisley, K. Medwid, N.P. Toltl, C.C. Chan, M. Skibic, K. Biswas, K.A. Wells, L.R. Snyder, J. Chromatogr. A 1101 (2006) 122.
[19] W.Z. Fan, Y. Zhang, P.W. Carr, S.C. Rutan, M. Dumarey, A.P. Schellinger, W. Pritts, J. Chromatogr. A 1216 (2009) 6587.
[20] D.M. Marchand, L.R. Snyder, J.W. Dolan, J. Chromatogr. A 1191 (2008) 2.
[21] J.W. Dolan, L.R. Snyder, J. Chromatogr. A 1216 (2009) 3467.
[22] M. Reta, P.W. Carr, P.C. Sadek, S.C. Rutan, Anal. Chem. 71 (1999) 3484.
[23] D. Visky, Y.V. Heyden, T. Ivanyi, P. Baten, J. De Beer, Z. Kovbacs, B. Moszal, P. Dehouck, E. Roets, D.L. Massart, J. Hoogmartens, J. Chromatogr. A 1012 (2003) 11.
[24] M.R. Euerby, P. Petersson, J. Chromatogr. A 994 (2003) 13.
[25] R. Kaliszan, J. Chromatogr. A 656 (1993) 417.
[26] J.G. Dorsey, J. Chromatogr. A 656 (1993) 485.
[27] N.S. Wilson, J.W. Dolan, L.R. Snyder, P.W. Carr, L.C. Sander, J. Chromatogr. A 961 (2002) 217.
[28] J.I. Siepmann, private communication.
[29] J.L. Rafferty, J.I. Siepmann, M.R. Schure, J. Chromatogr. A (2011) in press.
[30] J.P. Larmann, J.J. DeStefano, A.P. Goldberg, R.W. Stout, L.R. Snyder, M.A. Stadalius, J. Chromatogr. 255 (1983) 163.
[31] L.R. Snyder, J.J. Kirkland, J.W. Dolan, Introduction to Modern Liquid Chromatography, 3rd ed., Wiley-Interscience, New York, 2009 (Chapter 5).
[32] L.R. Snyder, A. Maule, A. Heebsch, R. Cuellar, S. Paulson, J. Carrano, L. Wrisley, C.C. Chan, N. Pearson, J.W. Dolan, J. Gilroy, J. Chromatogr. A 1057 (2004) 49.
[33] M. Kele, G. Guiochon, J. Chromatogr. A 960 (2002) 19.
[34] P.W. Carr, D.M. Martire, L.R. Snyder (Eds.), J. Chromatogr. A 656 (1993) 381.
[35] K.D. Lork, K.K. Unger, J.N. Kinkel, J. Chromatogr. 352 (1986) 199.
[36] L.C. Sander, S.A. Wise, J. Chromatogr. 316 (1984) 163.
[37] S.M. Staroverov, A.A. Serdan, G.V. Lisichkin, J. Chromatogr. 364 (1986) 377.
[38] P. van den Driest, H.J. Ritchie, Chromatographia 24 (1987) 324.
[39] J.L. Rafferty, Ph.D. Dissertation, University of Minnesota, 2009.
[40] M.R. Euerby, P. Petersson, W. Campbell, W. Roe, J. Chromatogr. A 1154 (2007) 138.
[41] D.H. Marchand, K. Croes, J.W. Dolan, L.R. Snyder, J. Chromatogr. A 1062 (2005) 57.
[42] D.H. Marchand, K. Croes, J.W. Dolan, L.R. Snyder, R.A. Henry, K.M.R. Kallury, S. Waite, J. Chromatogr. A 1062 (2005) 65.
[43] K. Croes, A. Steffens, D.H. Marchand, L.R. Snyder, J. Chromatogr. A 1098 (2005) 123.
[44] L.C. Sander, R.M. Parris, S.A. Wise, P. Garrigues, Anal. Chem. 63 (1991) 2589.
[45] L.C. Sander, S.A. Wise, Anal. Chem. 56 (1984) 504.
[46] N.S. Wilson, M.D. Nelson, J.W. Dolan, L.R. Snyder, P.W. Carr, J. Chromatogr. A 961 (2002) 195.
[47] J.L. Rafferty, J.I. Siepmann, M.R. Schure, J. Chromatogr. A 1216 (2009) 2320.